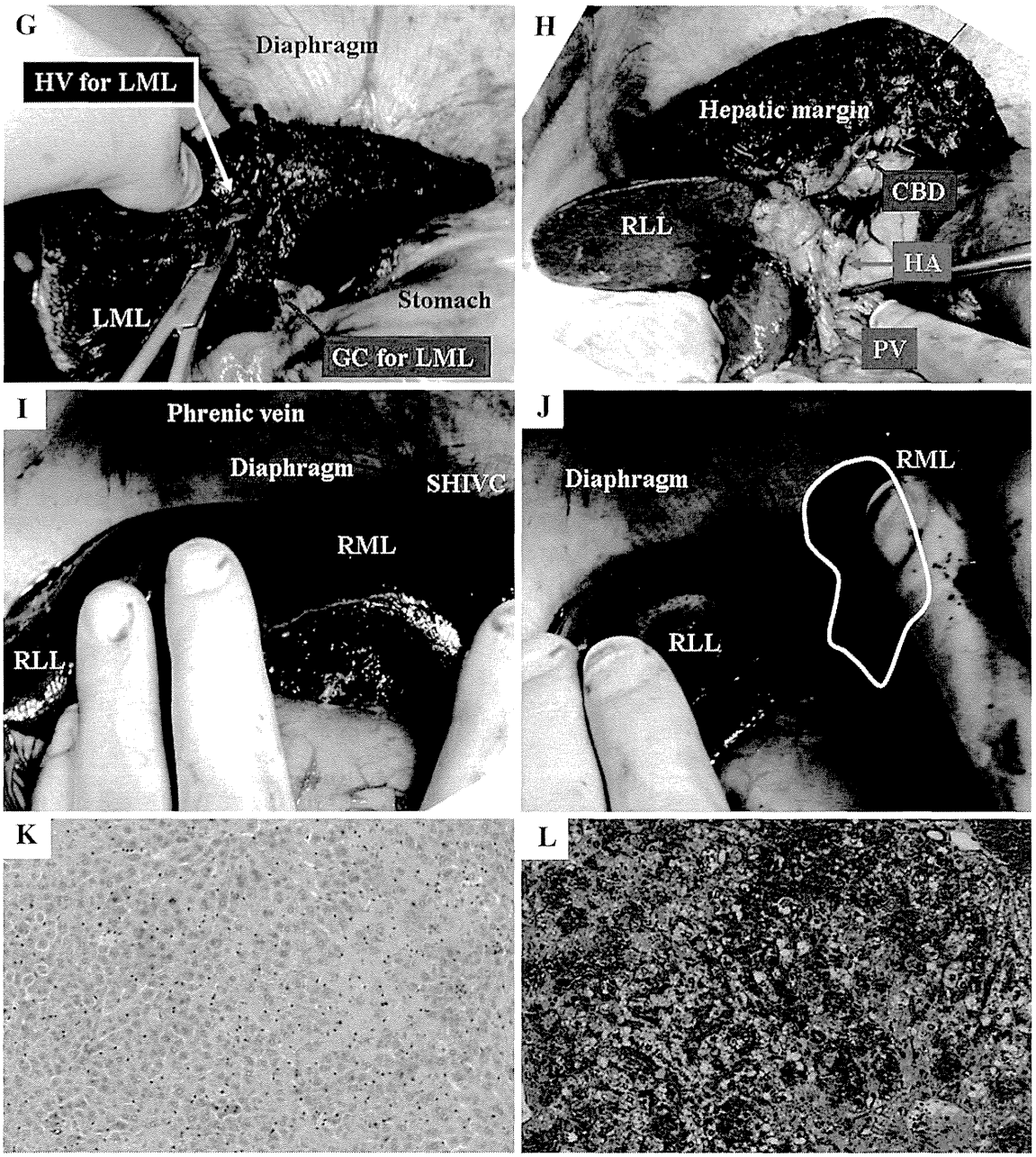

Fig. 4 continued

vary, although it is usually located on the PV trunk (Figs. 1, 3h, 4h). In the porcine liver, a demarcation line can be clearly observed after selective ligation of the HA branch (Fig. 3a, f, g). Selective temporal clamping of the HA branch of the RML and preceding confirmation of a related demarcation line on the RML are reasonable procedures to avoid unexpected obstruction of the HA flow to the RLL (Fig. 3e–g).

Anatomical variations are frequently found during surgery. Isolation of the HA branch to the RLL, skeletonization of the PV branch for the RML and preservation of the GC from the RLL to the CBD are keys in this model. The HA branch to the RLL is located above or behind the PV trunk. The PV branch for the RML diverges from the RPV or PV trunk. The GC from the RLL to the CBD is nestled in front of the PV branch for the RLL or is located between the PV branches for the RML and RLL.

The hanging maneuver is a technique used for passing a tape between the anterior surface of the inferior vena cava and the liver, which permits the liver to be suspended during parenchymal transection. The hepatic inferior vena cava and hepatic veins are completely covered by liver

parenchyma. Therefore, the hanging maneuver is difficult or impossible to perform in this model.

During liver resection, careless and blinded dissection of crossing tissues or vessels may result in unexpected injuries. To prevent any irrelevant damage to the liver remnant or grafts, we did not employ the Pringle maneuver in animal experiments, although the Pringle maneuver can be performed. Note that the GCs of the LML and LLL form dense tissues (Figs. 1, 2e, 3d, 4f), and that the HVs to the LML and LLL are located near each GC (Fig. 4g). For these reasons, we employ a two-step process (Fig. 4f) to skeletonize each GC to the LML and LLL. Although manual procedures using a crash method with adequate retraction are safe [8, 10] (Fig. 4c–e), the use of specially developed devices is helpful, especially for hemostasis [10–12]. We use an electrocautery scalpel and bipolar forceps with saline irrigation to ensure hemostasis [13, 14]. Subtle injuries of the cut surface and hepatic margin will cause intractable bleeding, especially in the RML close to the RLL. Note that the RML close to the RLL receives blood flow even after the ligations of the HA and PV branches to the RML (Fig. 4j). This is an important reason for an up-front confirmation of the demarcation line on the RML, even though other demarcation lines can be used for confirmation before ligations of the HA and PV branches.

The GCs of each lobe aggregate with the CBD at a relatively left side of the liver (Figs. 1, 2e, 3d), and the GCs from the RLL to CBD overlap with the critical vessels to the RML and RLL (Figs. 1, 2e, 3d, h). Moreover, there are various types of GC branches to the RLL, and we experienced a case with a GC branch to the RLL running at the RPV bifurcation to the RLL and RML. Therefore, selective ligation of the PV branch to the RML can involve technical difficulties, because subtle injuries to the GCs from the RLL to CBD should be avoided (Fig. 3h). However, from the viewpoints of an accurate functional liver volume and the control of hemostasis from the cut surface, selective ligation of the PV branch to the RML is crucial in this model.

An insufficient remnant in extended hepatectomy and a small-for-size graft in liver transplantation are important issues in the field of liver surgery [1]. Reliable and reproducible animal models that can provide clinically relevant data are required. We hope that our porcine model will be informative for researchers with an interest in liver surgery.

Acknowledgments We are grateful to Kentaro Taniguchi, Chiduru Yamamoto, Reo Sakakura and Kenji Nakamura (First Department of Surgery, Mie University Graduate School of Medicine, Tsu, Japan) for their support in establishing this model. This work was partially supported by a Grant-in-Aid for Scientific Research from the Japan Society for the Promotion of Science, Tokyo, Japan (MEXT/JSPS 24591877 to S. Yagi) and by a grant from the Uehara Memorial Foundation, Tokyo, Japan (No. 200940051 to T. Hori).

Conflict of interest None of the authors has any financial conflict of interest to declare.

References

1. Tucker ON, Heaton N. The 'small for size' liver syndrome. Curr Opin Crit Care. 2005;11:150–5.
2. Arkadopoulos N, Defterevos G, Nastos C, Papalois A, Kalimeris K, Papoutsidakis N, et al. Development of a porcine model of post-hepatectomy liver failure. J Surg Res. 2011;170:e233–42.
3. Xia Q, Lu TF, Zhou ZH, Hu LX, Ying J, Ding DZ, et al. Extended hepatectomy with segments I and VII as resection remnant: a simple model for small-for-size injuries in pigs. Hepatobiliary Pancreat Dis Int. 2008;7:601–7.
4. Goralczyk AD, Obed A, Beilage AG, Sattler B, Füzesi L, Lorf T. Tissue damage with different surgical techniques in a porcine model of liver resection: implications for living-donor liver transplantation? J Hepatobiliary Pancreat Sci. 2011;18:436–42.
5. Hori T, Yagi S, Iida T, Taniguchi K, Yamamoto C, Sakakura R, et al. Surgical text for orthotopic liver transplantation model with small-for-size graft in the pig: key techniques and pitfalls. Ann Gastroenterol. 2012;25:147–61.
6. Iida T, Yagi S, Taniguchi K, Hori T, Uemoto S. Improvement of morphological changes after 70 % hepatectomy with portocaval shunt: preclinical study in porcine model. J Surg Res. 2007;143:238–46.
7. Hanaoka J, Shimada M, Utsunomiya T, Morine Y, Imura S, Ikemoto T, Mori H. Significance of sonic hedgehog signaling after massive hepatectomy in a rat. Surg Today. 2013;43:300–7.
8. Ishizaki Y, Yoshimoto J, Sugo H, Miwa K, Kawasaki S. Hepatectomy using traditional Péan clamp-crushing technique under intermittent Pringle maneuver. Am J Surg. 2008;196:353–7.
9. Tanaka K, Inomata Y, Kaihara S. Surgical procedure for left lateral segmentectomy and left lobectomy. In: Tanaka K, Inomata Y, Kaihara S, editors. Living-donor liver transplantation: surgical techniques and innovations. 1st ed. Barcelona: Prous Science; 2003. p. 33–42.
10. Hori T, Yagi S, Iida T, Taniguchi K, Yamamoto C, Okamura Y, et al. Key techniques for orthotopic liver transplantation model with a 30 % graft in swine. Surg Today. 2013;43:1079–80.
11. Itoh S, Fukuzawa K, Shitomi Y, Okamoto M, Kinoshita T, Taketomi A, et al. Impact of the VIO system in hepatic resection for patients with hepatocellular carcinoma. Surg Today. 2012;42:1176–82.
12. Zhang S, Zheng Y, Wu B, Ji S, Yu Z, Zhang Q. Is the TissueLink dissecting sealer a better liver resection device than clamp-crushing? A meta-analysis and system review. Hepatogastroenterology. 2012;59:2602–8.
13. Yamamoto Y, Ikai I, Kume M, Sakai Y, Yamauchi A, Shinohara H, et al. New simple technique for hepatic parenchymal resection using a Cavitron Ultrasonic Surgical Aspirator and bipolar cautery equipped with a channel for water dripping. World J Surg. 1999;23:1032–7.
14. Tanaka K, Inomata Y, Kaihara S. Surgical procedure for left lateral segmentectomy and left lobectomy. In: Tanaka K, Inomata Y, Kaihara S, editors. Living-donor liver transplantation: surgical techniques and innovations. 1st ed. Barcelona: Prous Science; 2003. p. 67–74.

World Journal of Hepatology

Online Submissions: http://www.wjgnet.com/esps/
bpgoffice@wjgnet.com
doi:10.4254/wjh.v6.i72

World J Hepatol 2014 February 27; 6(2): 72-84
ISSN 1948-5182 (online)

ORIGINAL ARTICLE

Oxidative stress and extracellular matrices after hepatectomy and liver transplantation in rats

Tomohide Hori, Shinji Uemoto, Feng Chen, Lindsay B Gardner, Ann-Marie T Baine, Toshiyuki Hata, Takayuki Kogure, Justin H Nguyen

Tomohide Hori, Shinji Uemoto, Division of Hepato-Biliary-Pancreatic and Transplant Surgery, Department of Surgery, Kyoto University Graduate School of Medicine, Kyoto 606-8507, Japan
Feng Chen, Lindsay B Gardner, Ann-Marie T Baine, Toshiyuki Hata, Department of Neuroscience, Mayo Clinic, Jacksonville, FL 32224, United States
Takayuki Kogure, Department of Gastroenterology, Tohoku University Graduate School of Medicine, Sendai, Miyagi 980-8574, Japan
Justin H Nguyen, Division of Transplant Surgery, Department of Transplantation, Mayo Clinic, Jacksonville, FL 32224, United States
Author contributions: Hori T and Hata T performed the surgery and collected the data; Hori T wrote this paper; Chen F, Gardner LB and Baine AMT performed the assays; Kogure T helped to perform the protein assays; Nguyen JH and Uemoto S designed this study and supervised this research.
Supported by Grants to Nguyen JH from the Deason Foundation, Sandra and Eugene Davenport, Mayo Clinic CD CRT-II partially; the Uehara Memorial Foundation to Hori T, Tokyo 171-0033, Japan, No. 200940051
Correspondence to: Tomohide Hori, MD, PhD, Division of Hepato-Biliary-Pancreatic and Transplant Surgery, Department of Surgery, Kyoto University Graduate School of Medicine, 54 Shogoinkawara-cho, Sakyo-ku, Kyoto 606-8507, Japan. horit@kuhp.kyoto-u.ac.jp
Telephone: +81-75-7513111 Fax: +81-75-7513106
Received: July 30, 2013 Revised: December 8, 2013
Accepted: January 13, 2014
Published online: February 27, 2014

Abstract

AIM: To investigate oxidative stress (OS)-mediated damage and the behavior of extracellular matrices in various rat models because shear stress with portal hypertension and cold ischemia/warm reperfusion injury trigger the liver regeneration cascade after surgery. These injuries also cause fatal liver damage.

METHODS: Rats were divided into four groups according to the surgery performed: control; hepatectomy with 40% liver remnant (60% hepatectomy); orthotopic liver transplantation (OLT) with whole liver graft (100% OLT); and split OLT (SOLT) with 40% graft (40% SOLT). Survival was evaluated. Blood and liver samples were collected at 6 h after surgery. Biochemical and histopathological examinations were performed. OS-induced damage, 4-hydroxynonenal, ataxia-telangiectasia mutated kinase, histone H2AX, phosphatidylinositol 3-kinase (PI3K) and Akt were evaluated by western blotting. Behavior of extracellular matrices, matrix metalloproteinase (MMP)-9, MMP-2, tissue inhibitor of metalloproteinase (TIMP)-1 and TIMP-2 were also evaluated by western blotting and zymography.

RESULTS: Although 100% OLT survived, 60% hepatectomy and 40% SOLT showed poor survival. Histopathological, immunohistological, biochemical and protein assays revealed that 60% hepatectomy, 100% OLT and 40% SOLT showed liver damage. PI3K and Akt were decreased in 60% hepatectomy and 40% SOLT. For protein expression, 40% SOLT showed differences in MMP-9, MMP-2 and TIMP-2. TIMP-1 showed differences in 60% hepatectomy and 40% SOLT. For protein activity, MMP-9 demonstrated significant differences in 60% hepatectomy, 100% OLT and 40% SOLT.

CONCLUSION: Under conditions with an insufficient liver remnant, prevention of OS-induced damage *via* the Akt/PI3K pathway may be key to improve the postoperative course. MMP-9 may be also a therapeutic target after surgery.

Key words: Free radicals; Akt; Phosphatidylinositol 3-kinase; Matrix metalloproteinase; Tissue inhibitors of metalloproteinase

Core tip: Although shear stress with portal hypertension and cold ischemia/warm reperfusion injury trigger the liver regeneration cascade after surgery, these injuries also cause fatal liver damage. Postoperative liver damage is still a critical matter in the field of liver surgery. Oxidative stress and extracellular matrices are important for liver regeneration after surgery and these may be important keys to overcome current problems in the field of liver surgery. Here, we investigated oxidative stress-mediated damage and the behavior of extracellular matrices in various rat models with liver surgery.

Hori T, Uemoto S, Chen F, Gardner LB, Baine AMT, Hata T, Kogure T, Nguyen JH. Oxidative stress and extracellular matrices after hepatectomy and liver transplantation in rats. *World J Hepatol* 2014; 6(2): 72-84 Available from: URL: http://www.wjgnet.com/1948-5182/full/v6/i2/72.htm DOI: http://dx.doi.org/10.4254/wjh.v6.i2.72

INTRODUCTION

Liver resection is considered the standard treatment for primary malignant tumors and liver metastases. Advanced surgical techniques for hepatectomy, development of preoperative evaluation, and improvements in intensive postoperative care have resulted in a decline in perioperative morbidity and mortality. However, postoperative liver failure still occurs despite these developments. Extended hepatectomy has the advantage of high curability but increases morbidity and mortality[1]. Insufficient volume of the remnant liver is correlated with perioperative morbidity and mortality[1]. Prognosis of postoperative liver failure due to insufficient liver remnant is poor[1,2].

Orthotopic liver transplantation (OLT) is an accepted therapy for end-stage liver disease and currently provides long-term survival and good quality of life. However, cold ischemia/warm reperfusion (CIWR) injury is still a major cause of morbidity and mortality after OLT[3]. Currently, strategic procedures are needed to improve the liver tolerance against CIWR injury. A small-for-size graft (SFSG) is used for deceased donor liver transplantation (DDLT) and living donor liver transplantation (LDLT)[4,5]. The SFSG is defined as a ratio of graft weight against standard liver volume < 40%[6,7]. An inevitable insufficiency of graft size cannot be avoided in the LDLT or split orthotopic liver transplantation (SOLT) for DDLT. The SFSG in LDLT or SOLT is accompanied with CIWR injury and shear stress with portal hypertension. Hence, the SFSG results in high mortality and morbidity. The choice of a left-side graft is preferred from the viewpoint of greater donor safety and expanded donor candidates in LDLT[7,8]. Guaranteed SOLT with successful outcomes resolves a donor shortage in DDLT[4,5]. Currently, the 40% SFSG is a critical matter to overcome the donor shortage in DDLT and ensure donor safety in LDLT[4].

Oxygen is required for cell survival. However, it also poses a potential hazard *via* reactive oxygen species (ROS) and reactive nitrogen species (RNS), with biological and functional alterations of lipids, proteins and DNA[9-11]. Control of ROS/RNS production plays physiological roles, especially in regulating cell signaling, cell proliferation, differentiation and apoptosis[9-11]. Oxidative stress (OS) mediated by free radicals is defined as an imbalance between the production of ROS/RNS and the antioxidant capacity of the cell[9-11].

The extracellular matrix has important effects on inflammation, carcinogenesis and regeneration[12-14]. There are diverse types of proteases that control remodeling of the extracellular matrix, trigger liver regeneration and drive tumor progression[12-14]. Matrix metalloproteinases (MMPs) are a family of enzymes that degrade constituents of extracellular matrices and basement membranes. Currently, a total of 28 MMPs have been identified[14]. MMPs have been intensively studied and shown to play key roles in inflammation, carcinogenesis and regeneration[12-15]. MMP-2 and MMP-9 are implicated in liver injury and remodeling. In particular, previous researchers reported that MMP-9 and MMP-2 contribute to liver failure after liver surgery[12-21]. Tissue inhibitors of metalloproteinases (TIMPs) are a family of endogenous inhibitors of MMPs. Alteration in the MMP-TIMP balance is linked to pathophysiological conditions[22,23]. Currently, four members have been identified in the TIMP family which can inhibit various MMPs[24]. In particular, many researchers have focused on TIMP-1 and TIMP-2 during liver regeneration[25-28].

Although shear stress with portal hypertension and CIWR injury trigger the liver regeneration cascade after liver surgery, these injuries also cause fatal liver damage[29-31]. Initial damage is confirmed at the early postoperative period after liver surgery[3,12,13,18,29-31]. Therapeutic strategies to reduce this damage have the advantage of improving clinical results after liver surgery and overcoming the current issue of insufficient liver volume in the field of liver surgery. In the present preliminary study, we investigated OS-mediated damage and the behavior of extracellular matrices in various rat models with shear stress and portal hypertension and/or CIWR injury.

MATERIALS AND METHODS

Animals

Lewis rats (RT-1^l) were purchased from Harlan Laboratories (Indianapolis, IN, United States). Male rats were 8-12 wk old and weighed 250 g. The experimental protocols were approved by the Ethical Committee of our institution (Mayo Clinic, Institutional Animal Care and Use Committee, No. A19609). Rats were cared for in accordance with the Institutional Guidelines for Animal Welfare based on The National Institutes of Health Guide for the Care and Use of Laboratory Animals.

Surgical procedures and postoperative care

Comprehensive details of the surgical procedures for rat

Table 1 Study design

Group	Hepatic remnant volume	Cold ischemia warm reperfusion	Shear stress portal hypertension
Control	100%, native liver	-	-
60%-hepatectomy	40%, native liver	-	+
100%-OLT	100%, syngeneic graft	+	-
40%-SOLT	40%, syngeneic graft	+	+

OLT: Orthotopic liver transplantation; SOLT: Split orthotopic liver transplantation.

and postoperative care in our institution have been previously described[32-34]. In the hepatectomy model, 40% of liver remnant consisted of the left median and lateral segments[32,33]. In the transplantation model, the syngeneic graft had a cold ischemic time of 3-4 h at 4 ℃ in normal Ringer's solution[33]. The 40% SFSG was also formed by the left median and lateral segments at the back table[34]. To avoid any irrelevant signaling, the hepatic artery was reconstructed by ultramicrosurgery[33]. Each rat was kept separately after surgery and body temperature was maintained by a heating pad. Postoperative observation was performed every 30 min until 6 h after surgery and 1.0 mL of warm lactate Ringer's solution was routinely administered every 1 h until 6 h after surgery. In the transplantation model, we previously demonstrated the importance of a shortened anhepatic phase and exclusion of unreliable samples based on autopsy findings[33,34]. In this study, the anhepatic phase was kept within 20 min in the transplantation model. No surgical complications were observed in each case at sampling autopsy.

Study design

Rats were divided into four groups according to the surgery performed: (1) laparotomy only (control); (2) hepatectomy with 40% liver remnant (60% hepatectomy); (3) OLT with whole liver graft (100% OLT); and (4) SOLT with 40% SFSG (40% SOLT) (Table 1). The survival study was performed on 10 rats in each group. Cell signaling involved in proliferation, differentiation and apoptosis was confirmed at the early postoperative period after liver surgery and subsequently progressive necrosis was observed, as described previously[3,12,13,18,29-31]. Serum and plasma were collected at 6 h after surgery (n = 5, in each group). Liver samples were also collected at 6 h after surgery for histopathological/immunohistological assessments, western blotting and gelatin zymography (n = 5, in each group).

Biochemical assays and coagulation profile

Aspartate aminotransferase (AST), alanine aminotransferase (ALT), total bilirubin (T-Bil), the international normalized ratio of prothrombin time (PT-INR) and hyaluronic acid (HA) were measured. Serum AST, ALT and T-Bil were assessed by commercial kits (SGOT, SGPT and total bilirubin reagent, respectively; Biotron, Hemet, CA, United States). The PT-INR in the plasma was measured by the i-STAT System (Abbott, Princeton, NJ, United States). Serum HA was measured using a commercial kit (Quantikine Hyaluronan ELISA Kit; R and D Systems, Minneapolis, MN, United States).

Histopathological and immunohistological assessments

Liver tissue was fixed in 10% neutral-buffered formalin, embedded in paraffin, and sliced into 4-μm sections. The morphological characteristics and graft injury scores were assessed after hematoxylin-eosin (HE) staining. The graft damage score has been described previously[34]. Scores were counted in 10 fields (× 100 magnification) in each slide and these scores were averaged in each HE slide.

Induction of apoptosis was assessed by immunostaining of terminal deoxynucleotidyl transferase-mediated deoxyuridine triphosphate nick-end labeling (TUNEL) (ApopTag Peroxidase *In Situ* Apoptosis Detection Kit, S7100; Chemicon International, Billerica, MA, United States) and cysteine aspartic acid protease (caspase) 3 [Cleaved Caspase-3 (Asp175) Antibody, 9661S; Cell Signaling Technology, Danvers, MA, United States]. A TUNEL-positive nucleus was stained brown and a negative nucleus was counterstained light blue. A caspase-3-positive nucleus was stained brown and a negative nucleus was counterstained blue. Slides were scanned with an automated high-throughput scanning system (Scanscope XT, Aperio Technologies, Vista, CA, United States). To quantify the immunohistological findings, positive-stained nuclei were counted by Aperio Imagescope software (Aperio Technologies). All nuclei were classified into four color intensity levels and the higher two levels were considered as positive. The ratio of positive-stained nuclei to all nuclei was calculated and the mean ratio/mm^2 was determined.

Western blotting and gelatin zymography

The primary antibodies for malondialdehyde (MDA) (Anti-Malondialdehyde antibody, ab6463; Abcam, Cambridge, MA, United States); 4-hydroxynonenal (4-HNE) (4 Hydroxynonenal antibody, ab46545; Abcam); ataxia telangiectasia mutated kinase (ATM) (Phospho-ATM/ATR Substrate Rabbit mAb, 2909; Cell Signaling Technology); phosphorylated histone H2AX (γH2AX) (Phospho-Histone H2A.X Antibody, 2577; Cell Signaling Technology); phosphatidylinositol 3-kinase (PI3K) (Phospho-PI3K p85/p55 Antibody, 4228; Cell Signaling Technology); Akt (Phospho-Akt Rabbit mAb, 4058; Cell Signaling Technology); superoxide dismutase (SOD) (Cu/Zn Superoxide Dismutase, LS-B2907; LifeSpan BioSciences, Seattle, WA, United States); catalase (Catalase, LS-B2554; LifeSpan BioSciences); MMP-9 (Anti-MMP-9, Catalytic domain, AB19016; Millipore, Temecula, CA,

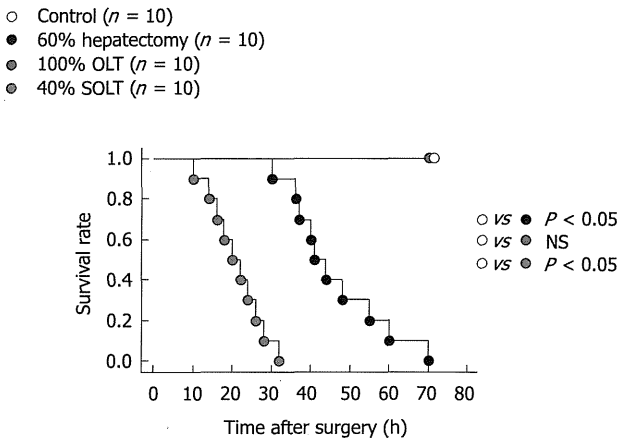

Figure 1 Survival curves. OLT: Orthotopic liver transplantation; SOLT: Split orthotopic liver transplantation.

United States); MMP-2 [MMP-2 antibody (MMP2/8B4), ab7032; Abcam]; TIMP-1 [Anti-TIMP-1 Mouse mAb (102D1), IM63; Calbiochem, San Diego, CA, United States]; and TIMP-2 [Anti-TIMP2 antibody (3A4), ab1828; Abcam] were used. Glyceraldehyde-3-phosphate dehydrogenase served as a control. Signals were quantified using ImageQuant 5.0 software (Molecular Dynamics, Sunnyvale, CA, United States). Gelatinase activity was visualized by fluorescence microscopy (Olympus BX50; Olympus Optical, Tokyo, Japan).

Statistical analysis

The results were presented as mean ± SD. Student's *t* test was used for the comparison of unpaired continuous variables between groups. Survival curves were constructed by the Kaplan-Meier method (Log-rank test). Statistical calculations were performed using SPSS version 16.0 (SPSS Inc., Chicago, IL, United States). $P < 0.05$ was considered statistically significant.

RESULTS

Survival curves

Survival curves for each group are shown in Figure 1. All rats that underwent a laparotomy or 100% OLT survived. The 60% hepatectomy and 40% SOLT groups clearly showed poorer survival than the controls ($P < 0.0001$). Insufficient liver remnant resulted in poor survivals after 60% hepatectomy. Especially, 40% SOLT showed very poor survivals.

Liver parenchymal damage

In comparison with the controls (0.1 ± 0.1 points), there were significant differences in the graft damage score for 60% hepatectomy (3.7 ± 0.7 points, $P < 0.0001$), 100% OLT (4.0 ± 0.6 points, $P < 0.0001$) and 40% SOLT (5.8 ± 1.1 points, $P < 0.0001$) (Figure 2A).

Immunohistological assessment of apoptosis induction

In comparison with the controls (0.003 ± 0.004), the rates of TUNEL-positive nuclei showed significant differences in 60% hepatectomy (0.017 ± 0.009, $P = 0.0278$), 100% OLT (0.107 ± 0.012, $P = 0.0001$) and 40% SOLT (0.166 ± 0.052, $P < 0.0001$) (Figure 2B). In comparison with the controls (0.002 ± 0.002), the rates of caspase-3-positive nuclei revealed significant differences in 60% hepatectomy (0.044 ± 0.023, $P = 0.0033$), 100% OLT (0.063 ± 0.014, $P < 0.0001$) and 40% SOLT (0.115 ± 0.019, $P < 0.0001$) (Figure 2C).

Conventional liver function tests, coagulation profile and endothelial damage

In comparison with the controls (42.5 ± 8.6 U/L), AST levels showed significant differences in 60% hepatectomy (202.4 ± 41.9 U/L, $P < 0.0001$), 100% OLT (290.5 ± 31.9 U/L, $P < 0.0001$) and 40% SOLT (387.4 ± 36.8 U/L, $P < 0.0001$) (Figure 3A). In comparison with the controls (59.8 ± 9.6 U/L), ALT levels showed significant differences in 60% hepatectomy (213.8 ± 57.0 U/L, $P < 0.0001$), 100% OLT (309.4 ± 38.3 U/L, $P < 0.0001$) and 40% SOLT (392.2 ± 76.7 U/L, $P < 0.0001$) (Figure 3B). In comparison with the controls (0.41 ± 0.13 mg/dL), there were no significant differences in T-Bil levels in 60% hepatectomy (0.50 ± 0.26 mg/dL, $P = 0.4798$) and 100% OLT (0.58 ± 0.15 mg/dL, $P = 0.0801$), but there was in 40% SOLT (1.37 ± 0.29 mg/dL, $P = 0.0001$) (Figure 3C).

In comparison with the controls (0.99 ± 0.04), PT-INR values revealed significant differences in 60% hepatectomy (1.16 ± 0.09, $P = 0.0052$), 100% OLT (1.12 ± 0.04, $P = 0.0008$) and 40% SOLT (1.22 ± 0.06, $P < 0.0001$) (Figure 3D).

In comparison with the controls (76.6 ± 14.9 ng/mL), HA levels demonstrated significant differences in 60% hepatectomy (264.0 ± 58.8 mg/dL, $P = 0.0001$), 100% OLT (188.0 ± 29.0 mg/dL, $P < 0.0001$) and 40% SOLT (350.2 ± 136.6 mg/dL, $P = 0.0021$) (Figure 3E).

Oxidative stress

The western blotting intensities of MDA in each group are shown in Figure 4A. In comparison with the controls (1.00 ± 0.10), normalized MDA showed significant differences in 60% hepatectomy (1.64 ± 0.39, $P = 0.0074$), 100% OLT (2.12 ± 0.78, $P = 0.0133$) and 40% SOLT (2.30 ± 0.26, $P < 0.0001$) (Figure 4B).

Lipid peroxidation

In comparison with the controls (1.00 ± 0.09), normalized 4-HNE showed significant differences in 60% hepatectomy (1.30 ± 0.20, $P = 0.0152$), 100% OLT (1.41 ± 0.20, $P = 0.0028$) and 40% SOLT (1.40 ± 0.19, $P = 0.0032$) (Figure 4C).

Responses and repairs to DNA damage

In comparison with the controls (1.00 ± 0.098), normalized ATM showed significant differences in 60% hepatectomy (1.15 ± 0.09, $P = 0.0336$), 100% OLT (1.28 ± 0.10, $P = 0.0015$) and 40% SOLT (1.21 ± 0.09, $P = 0.0053$) (Figure 4D). In comparison with the controls (1.00 ± 0.17), normalized γH2AX showed significant differences

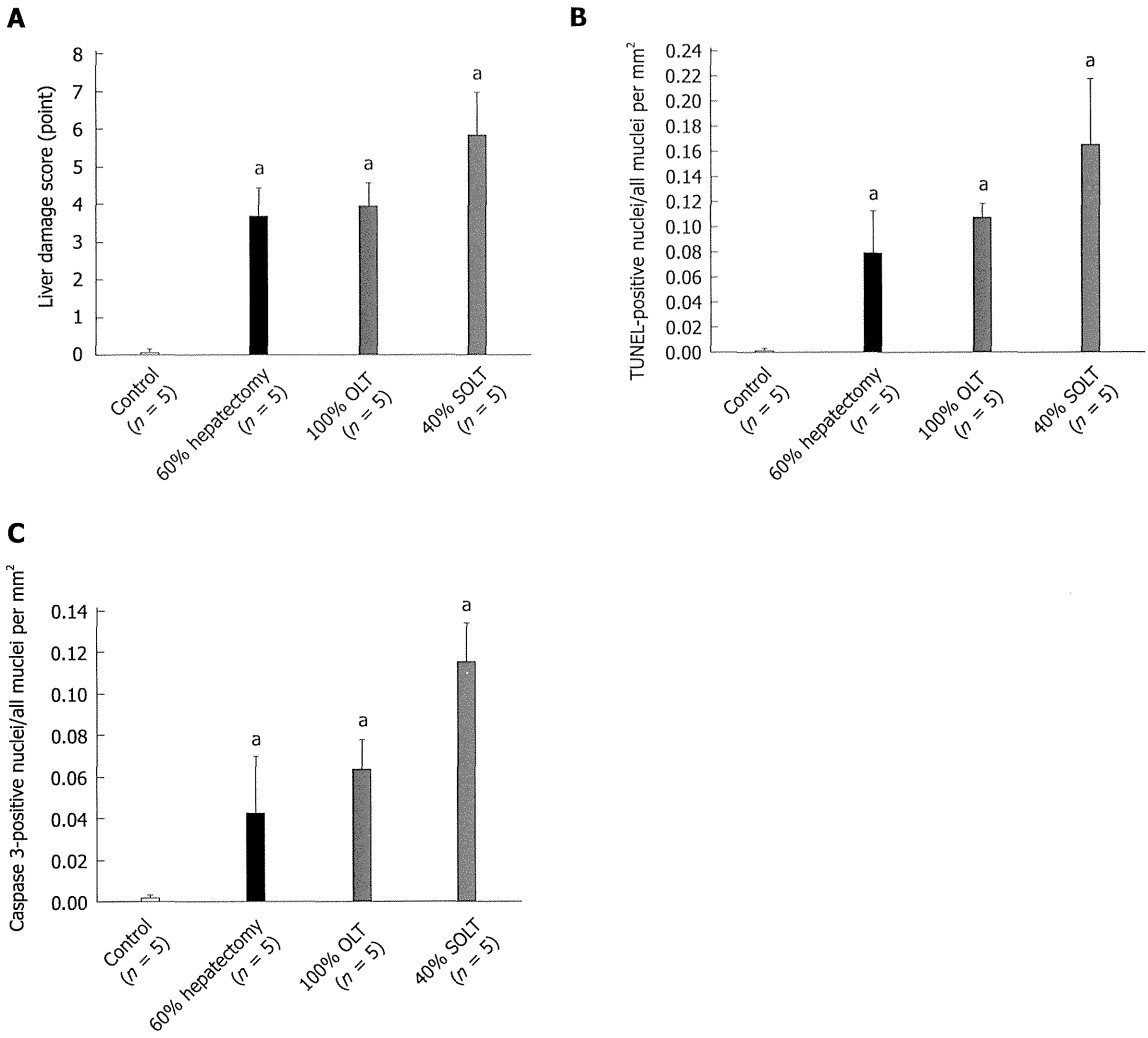

Figure 2 Histopathological and immunohistological assessments. A: Liver damage score in HE staining; B: TUNEL-positive rate; C: Caspase-3-positive rate. [a]$P < 0.05$ *vs* control. OLT: Orthotopic liver transplantation; SOLT: Split orthotopic liver transplantation.

in 60% hepatectomy (1.39 ± 0.29, $P = 0.0071$), 100% OLT (1.67 ± 0.38, $P = 0.0303$) and 40% SOLT (2.59 ± 0.66, $P = 0.0008$) (Figure 4E).

Promotion of cell survival

The western blotting intensities of PI3K and Akt in each group are shown in Figure 4F.

In comparison with the controls (1.00 ± 0.08), there was no significant difference in normalized PI3K in 100% OLT (0.92 ± 0.09, $P = 0.1726$), but there were significant differences in 60% hepatectomy (00.36 ± 0.11, $P < 0.0001$) and 40% SOLT (0.42 ± 0.19, $P = 0.0002$) (Figure 4G). In comparison with the controls (1.00 ± 0.12), there was no significant difference in normalized Akt in 100% OLT (0.92 ± 0.37, $P = 0.6486$), but there were significant differences in 60% hepatectomy (0.37 ± 0.23, $P = 0.0007$) and 40% SOLT (0.34 ± 0.24, $P = 0.0006$) (Figure 4H).

Activities of antioxidant enzymes

In comparison with the controls (1.00 ± 0.09), normalized SOD did not show significant differences in 60% hepatectomy (0.97 ± 0.09, $P = 0.6503$), 100% OLT (0.96 ± 0.11, $P = 0.5461$) and 40% SOLT (0.87 ± 0.09, $P = 0.0595$) (Figure 4I). In comparison with the controls (1.00 ± 0.17), normalized catalase also revealed no significant differences in 60% hepatectomy (0.91 ± 0.11, $P = 0.3665$), 100% OLT (0.90 ± 0.15, $P = 0.3365$) and 40% SOLT (0.95 ± 0.14, $P = 0.6454$) (Figure 4J).

Behavior of MMP-9, MMP-2, TIMP-1 and TIMP-2

Protein expression and activity of MMP-9 are shown in Figure 5A. Protein expression was evaluated by western blot densitometry (Figure 5B-D). In comparison with the controls (1.00 ± 0.34), there were no significant differences in normalized MMP-9 in 60% hepatectomy (1.14 ± 0.43, $P = 0.5811$) and 100% OLT (1.18 ± 0.35, $P = 0.4254$), but there was a significant difference in 40% SOLT (2.16 ± 0.26, $P = 0.0003$) (Figure 5B). In comparison with the controls (1.00 ± 0.16), there were no significant differences in normalized MMP-2 in 60% hepatectomy (0.78 ± 0.17, $P = 0.0716$) and 100% OLT (0.80 ± 0.23, $P = 0.1437$), but there was a significant difference in 40% SOLT (0.78 ± 0.12, $P = 0.0385$) (Figure

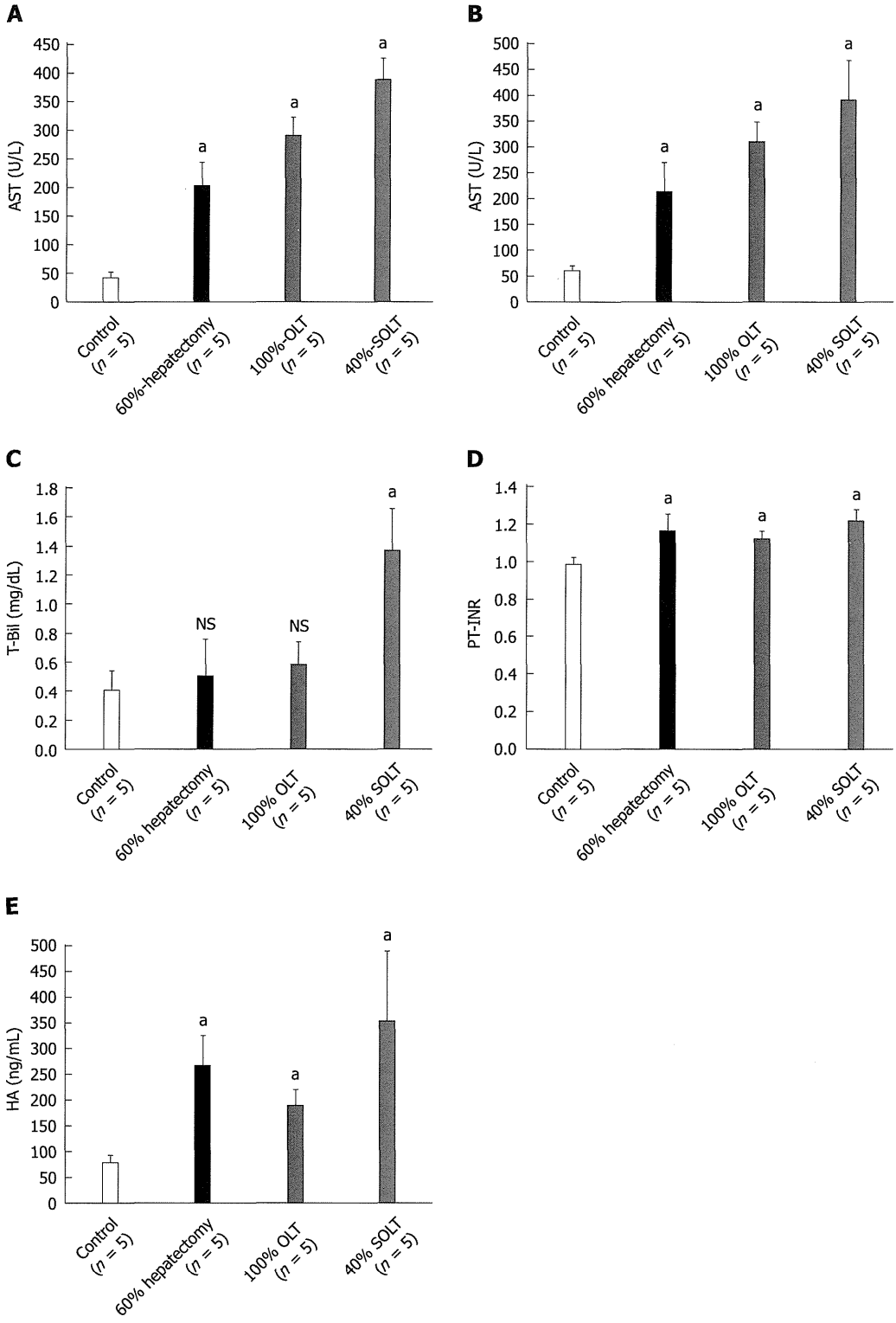

Figure 3 Biochemical and coagulation profiles. A: Serum aspartate aminotransferase (AST); B: Serum alanine aminotransferase (ALT); C: Serum total bilirubin (T-Bil); D: Plasma international normalized ratio of prothrombin time (PT-INR); E: Serum hyaluronic acid (HA). $^{a}P < 0.05$ *vs* control. NS: Not significant ($P \geq 0.05$); OLT: Orthotopic liver transplantation; SOLT: Split orthotopic liver transplantation.

5C). In comparison with the controls (1.00 ± 0.30), there was no significant difference in normalized TIMP-1 in 100% OLT (0.82 ± 0.43, $P = 0.4654$), but there were significant differences in 60% hepatectomy (1.41 ± 0.26, $P = 0.0491$) and 40% SOLT (1.46 ± 0.32, $P = 0.0486$) (Figure 5D). In comparison with the controls (1.00 ± 0.24), there were no significant differences in normalized TIMP-2 in 60% hepatectomy (1.23 ± 0.24, $P = 0.1605$) and 100% OLT (0.95 ± 0.17, $P = 0.6846$), but there was a significant difference in 40% SOLT (1.28 ± 0.12, $P = 0.0471$) (Figure 5E).

Protein activities were evaluated by intensity in zy-

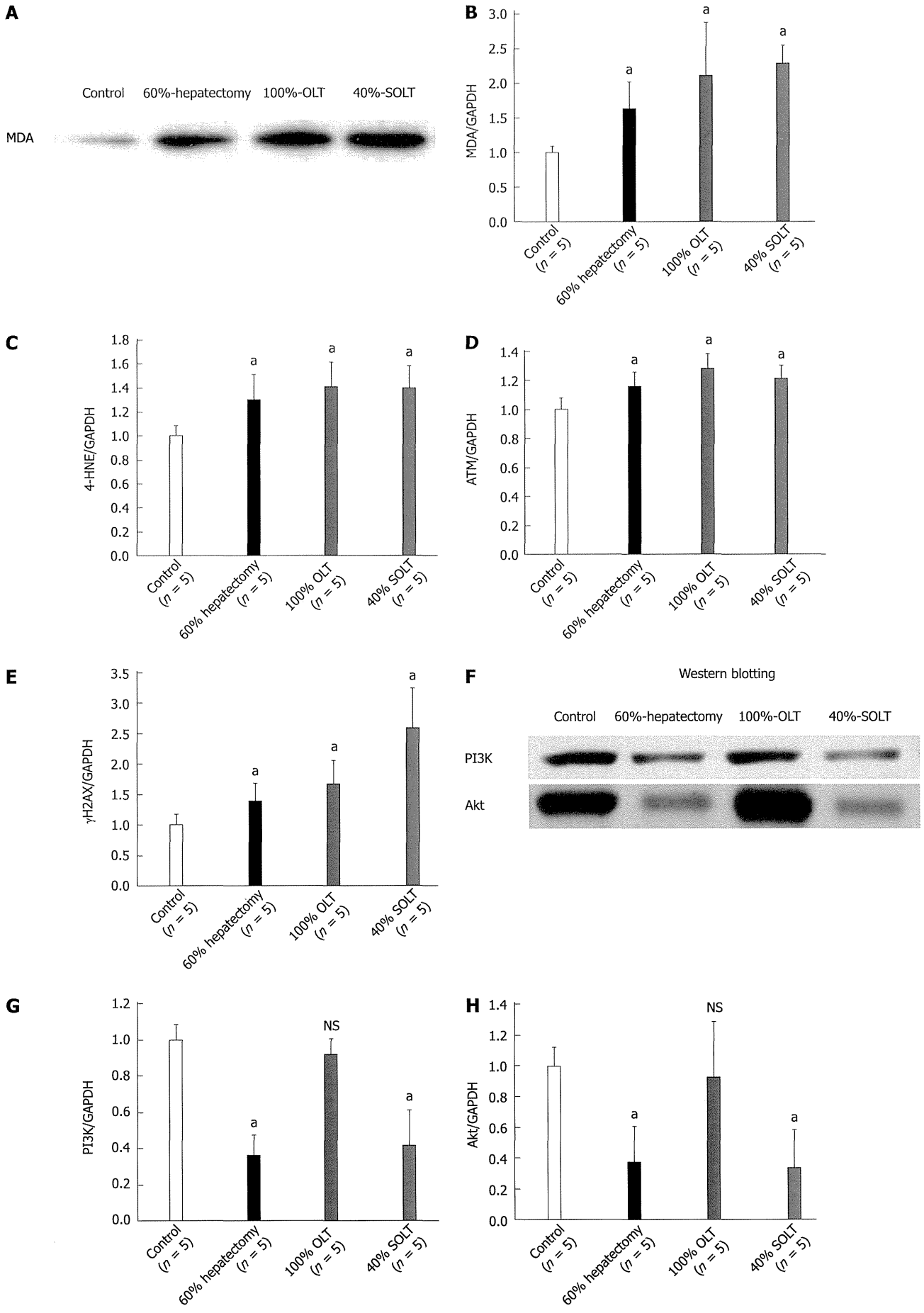
A
Control
60%-hepatectomy
100%-OLT
40%-SOLT
MDA
B
MDA/GAPDH
C
4-HNE/GAPDH
D
ATM/GAPDH
E
γH2AX/GAPDH
F
Western blotting
Control
60%-hepatectomy
100%-OLT
40%-SOLT
PI3K
Akt
G
PI3K/GAPDH
H
Akt/GAPDH
NS
a
Control (n = 5)
60% hepatectomy (n = 5)
100% OLT (n = 5)
40% SOLT (n = 5)

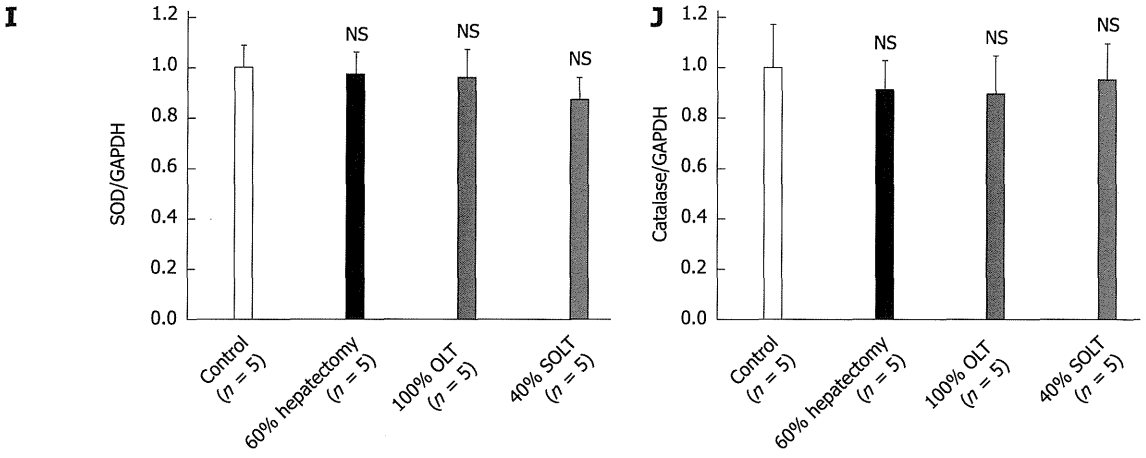

Figure 4 Protein expression of malondialdehyde, 4-hydroxynonenal, ataxia-telangiectasia mutated kinas/H2AX, phosphatidylinositol 3-kinase/Akt and antioxidant enzymes. A: Actual intensities of malondialdehyde (MDA) in western blotting; B: Normalized MDA; C: Normalized 4-hydroxynonenal (4-HNE); D: Normalized ataxia-telangiectasia mutated kinase (ATM); E: Normalized γH2AX; F: Actual intensities of phosphatidylinositol 3-kinase (PI3K) and Akt in western blotting; G: Normalized PI3K; H: Normalized Akt; I: Normalized superoxide dismutase (SOD); J: Normalized catalase. $^{a}P < 0.05$ *vs* control. NS: Not significant ($P \geq 0.05$); OLT: Orthotopic liver transplantation; SOLT: Split orthotopic liver transplantation.

mography (Figure 5F-I). In comparison with the controls (1.00 ± 0.15), relative MMP-9 clearly demonstrated significant differences in 60% hepatectomy (1.37 ± 0.23, $P = 0.0156$), 100% OLT (1.47 ± 0.33, $P = 0.0211$) and 40% SOLT (2.10 ± 0.75, $P = 0.0125$) (Figure 5F). In comparison with the controls (1.00 ± 0.17), relative MMP-2 did not reveal significant differences in 60% hepatectomy (1.03 ± 0.12, $P = 0.7444$), 100% OLT (0.98 ± 0.15, $P = 0.8821$) and 40% SOLT (1.04 ± 0.13, $P = 0.6847$) (Figure 5G). In comparison with the controls (1.00 ± 0.15), relative TIMP-1 did not reveal significant differences in 60% hepatectomy (0.96 ± 0.29, $P = 0.7926$), 100% OLT (0.98 ± 0.09, $P = 0.8217$) and 40% SOLT (0.91 ± 0.26, $P = 0.5347$) (Figure 5H). In comparison with the controls (1.00 ± 0.12), relative TIMP-2 did not show significant differences in 60% hepatectomy (1.04 ± 0.09, $P = 0.5974$), 100% OLT (1.03 ± 0.11, $P = 0.6845$) and 40% SOLT (1.03 ± 0.16, $P = 0.7495$) (Figure 5I).

Statistical differences between groups

As described above, the data in comparisons with the controls are shown. Statistical differences between groups are summarized in Table 2.

DISCUSSION

In survival and histopathological studies, 40% SOLT involved dual damage (*i.e.*, shear stress with portal hypertension and CIWR injury) and showed the poorest survival and most severe liver damage. Although 100% OLT showed good survival, CIWR injury was observed by histopathological and biochemical findings. Here, we used plasma PT-INR and serum HA levels as markers of sinusoidal endothelial damage and all groups showed significant differences. Survival in the 60% hepatectomy and 40% SOLT groups seemed to be higher than in the 100% OLT group and this may reflect the damage induced by shear stress and portal hypertension. Our histopathological, immunohistological and biochemical findings revealed that liver damage and apoptotic induction were observed in the early postoperative period after liver surgery, as in previous studies[3,12,13,18,29-31]. Paradoxically, the early postoperative period may have a therapeutic potential for a subsequent course after liver surgery.

OS causes DNA damage and subsequent apoptosis and is an imbalance between production of free radicals and antioxidant defenses[9-11]. From the viewpoint of production of free radicals, ROS/RNS can attack and damage a variety of critical biological molecules, including lipids, essential cellular proteins and DNA[9-11]. Products of lipid peroxidation can be easily detected in biological fluids and tissues and can reliably and rapidly reflect the sensitive and specific signals of lipid peroxidation that occur *in vivo*[35,36]. The compound 4-HNE is an end product of lipoperoxidation with antiproliferative and proapoptotic properties[35,36]. Our results with MDA and 4-HNE confirmed that OS occurred even in the early postoperative period.

With regard to DNA damage responses, the protein kinase ATM can be initiated through rapid intermolecular autophosphorylation induced by DNA damage, phosphorylate various proteins and subsequently amplify the responses to DNA damage[36,37]. This DNA damage-inducible kinase activates H2AX[38]. H2AX is required for cell cycle arrest and DNA repair following double-stranded DNA breaks[38,39]. DNA damage results in the rapid phosphorylation of H2AX by ATM[38,40]. Within minutes of DNA damage, H2AX is phosphorylated at the sites of the DNA damage[38]. This early event in the DNA-damage response is required for the recruitment of many DNA-damage response proteins. Therefore, histone H2AX is activated by ATM after DNA dam-

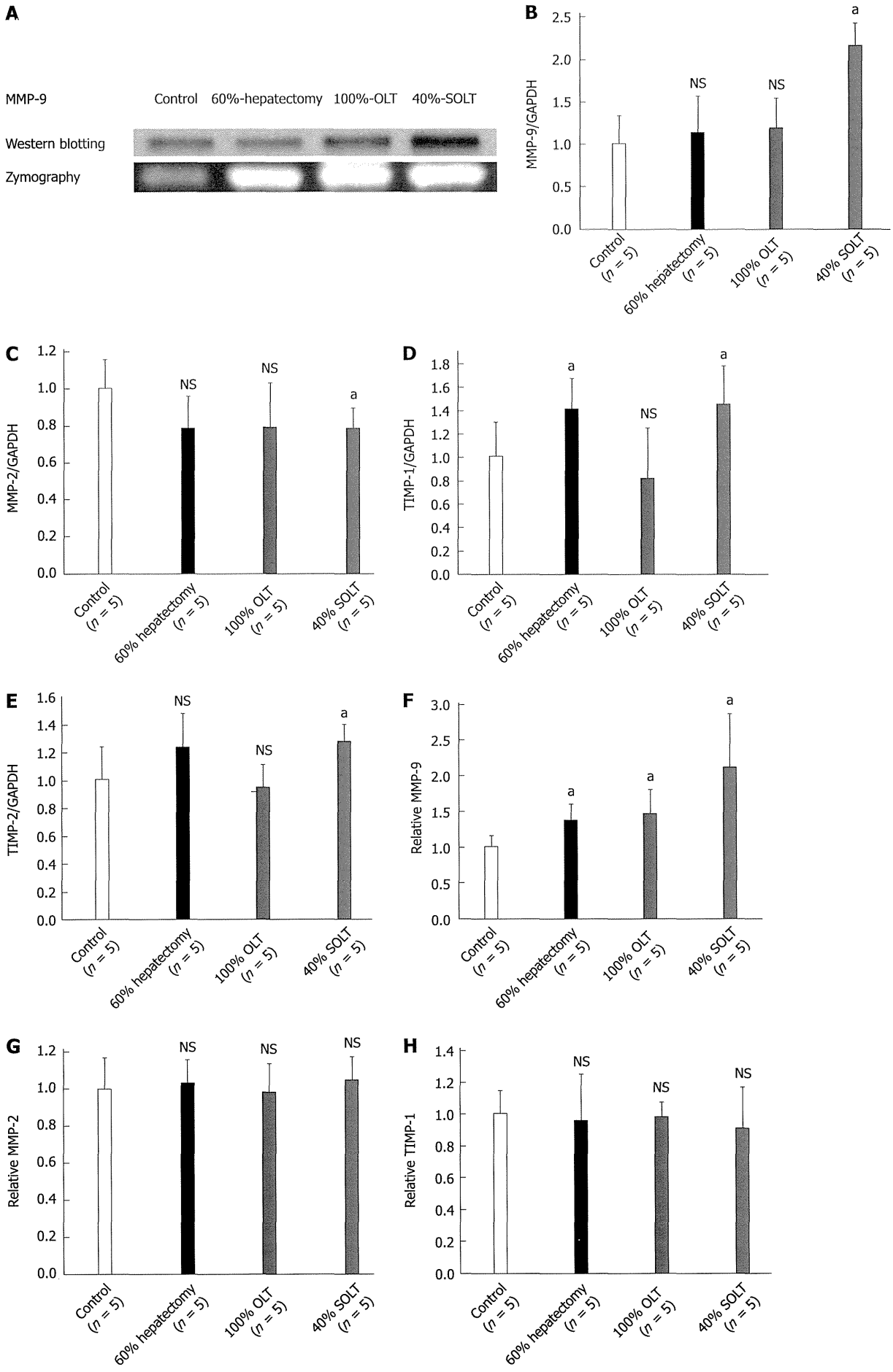
A
MMP-9
Control
60%-hepatectomy
100%-OLT
40%-SOLT
Western blotting
Zymography
B
MMP-9/GAPDH
NS
NS
a
C
MMP-2/GAPDH
NS
NS
a
D
TIMP-1/GAPDH
a
NS
a
E
TIMP-2/GAPDH
NS
NS
a
F
Relative MMP-9
a
a
a
G
Relative MMP-2
NS
NS
NS
H
Relative TIMP-1
NS
NS
NS
Control (n = 5)
60% hepatectomy (n = 5)
100% OLT (n = 5)
40% SOLT (n = 5)

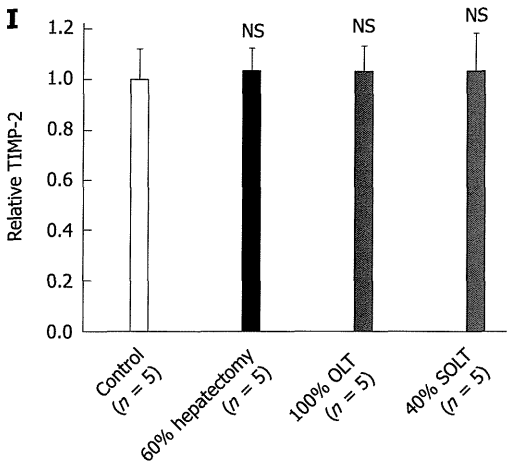

Figure 5 Protein expression and activities of matrix metalloproteinases and tissue inhibitor of metalloproteinases. A: Actual protein expression and activities of matrix metalloproteinase (MMP)-9; B: Normalized MMP-9; C: Normalized MMP-2; D: Normalized tissue inhibitor of metalloproteinase (TIMP)-1; E: Normalized TIMP-2; F: Relative MMP-9; G: Relative MMP-2; H: Relative TIMP-1; I: Relative TIMP-2. $^{a}P < 0.05$ *vs* control. NS: Not significant ($P \geqslant 0.05$); OLT: Orthotopic liver transplantation; SOLT: Split orthotopic liver transplantation.

Table 2 Statistical differences between groups

	Control *vs* 60%-hepatectomy	Control *vs* 100%-OLT	Control *vs* 40%-SOLT	60%-hepatectomy *vs* 100%-OLT	60%-hepatectomy *vs* 40%-SOLT	100%-OLT *vs* 40%-SOLT
Survival rate	$P < 0.05$	NS	$P < 0.05$	$P < 0.05$	$P < 0.05$	$P < 0.05$
Liver damage score	$P < 0.05$	$P < 0.05$	$P < 0.05$	NS	$P < 0.05$	$P < 0.05$
TUNEL positive ratio	$P < 0.05$	$P < 0.05$	$P < 0.05$	$P < 0.05$	$P < 0.05$	$P < 0.05$
Caspase-3 positive ratio	$P < 0.05$	$P < 0.05$	$P < 0.05$	$P < 0.05$	$P < 0.05$	$P < 0.05$
AST	$P < 0.05$	$P < 0.05$	$P < 0.05$	$P < 0.05$	$P < 0.05$	$P < 0.05$
ALT	$P < 0.05$	$P < 0.05$	$P < 0.05$	$P < 0.05$	$P < 0.05$	NS
T-Bil	NS	NS	$P < 0.05$	NS	$P < 0.05$	$P < 0.05$
PT-INR	$P < 0.05$	p <0.05	$P < 0.05$	$P < 0.05$	$P < 0.05$	$P < 0.05$
HA	$P < 0.05$	p <0.05	$P < 0.05$	$P < 0.05$	$P < 0.05$	$P < 0.05$
Western blotting						
MDA	$P < 0.05$	$P < 0.05$	$P < 0.05$	NS	$P < 0.05$	NS
4-HNE	$P < 0.05$	$P < 0.05$	$P < 0.05$	NS	NS	NS
ATM	$P < 0.05$	$P < 0.05$	$P < 0.05$	NS	NS	NS
γH2AX	$P < 0.05$	$P < 0.05$	$P < 0.05$	NS	$P < 0.05$	$P < 0.05$
PI3K	$P < 0.05$	NS	$P < 0.05$	$P < 0.05$	NS	$P < 0.05$
Akt	$P < 0.05$	NS	$P < 0.05$	$P < 0.05$	NS	$P < 0.05$
SOD	NS	NS	NS	NS	NS	NS
Catalase	NS	NS	NS	NS	NS	NS
MMP-9	NS	NS	$P < 0.05$	NS	$P < 0.05$	$P < 0.05$
MMP-2	NS	NS	$P < 0.05$	NS	NS	NS
TIMP-1	$P < 0.05$	NS	$P < 0.05$	$P < 0.05$	NS	$P < 0.05$
TIMP-2	NS	NS	$P < 0.05$	$P < 0.05$	NS	$P < 0.05$
Zymography						
MMP-9	$P < 0.05$	$P < 0.05$	$P < 0.05$	NS	$P < 0.05$	p <0.05
MMP-2	NS	NS	NS	NS	NS	NS
TIMP-1	NS	NS	NS	NS	NS	NS
TIMP-2	NS	NS	NS	NS	NS	NS

OLT: Orthotopic liver transplantation; SOLT: Split orthotopic liver transplantation; AST: Aspartate aminotransferase; ALT: Alanine aminotransferase; T-Bil: Total bilirubin; PT-INR: International normalized ratio of prothrombin time; HA: Hyaluronic acid; MDA: Malondialdehyde; 4-HNE: 4-hydroxynonenal; ATM: Ataxia-telangiectasia mutated kinase; PI3K: Phosphatidylinositol 3-kinase; SOD: Superoxide dismutase; MMP: Matrix metalloproteinase; TIMP: Tissue inhibitor of metalloproteinase.

age[38]. Thus, the ATM/H2AX signaling pathway is important in the response to and repair of DNA damage induced by OS[38,41]. Our results with ATM and H2AX clearly showed that OS after liver surgery caused DNA damage signaling and triggered subsequent DNA repair. In this study, groups with only CIWR injury (*i.e.*, 100% OLT) caused OS-induced damage and subsequent apoptotic process. However, this group showed differences not in PI3K/Akt, but in ATM/H2AX. These results suggested that CIWR injury induce apoptosis due to OS *via* the ATM/H2AX pathway.

Akt also plays a critical role in controlling apoptosis

and promotes cell survival to prohibit apoptosis[42-44]. Apoptotic machinery is inhibited by the activation of Akt[42-44]. Akt is an integral component of the antiapoptotic process related to the activation of PI3K[42-45]. Our results clearly showed that groups with accompanying shear stress and portal hypertension (*i.e.*, 60% hepatectomy and 40% SOLT) had decreased PI3K and Akt. This suggested that a subsequent apoptotic process was triggered in these groups. Shear stress and portal hypertension due to insufficient liver volume induce apoptosis due to OS *via* the Akt/PI3K pathway.

With regard to antioxidant defense, scavenging enzymes of free radicals, such as SOD and catalase, also play an important role in reducing DNA damage and subsequent apoptosis[10,11]. Cells are normally able to defend themselves against OS-induced damage through this scavenging system[10,11]. Our results revealed that this scavenging system did not appear to be triggered, although these scavenging enzymes can cope with large amounts of ROS[46]. Shear stress with portal hypertension and/or CIWR injury after liver surgeries in this study caused considerable liver damage. A possible explanation is that this scavenging system failed to stimulate some reactive molecules because of considerable damage after liver surgery.

MMPs have been intensively studied and shown to play key roles in inflammation, carcinogenesis and regeneration and many researchers have already focused on MMP-2 and MMP-9 after liver surgery[12-21]. In the present study, 40% SOLT increased protein expression of MMP-2 in western blotting, although zymography did not show any differences. Contrary to MMP-2, postoperative MMP-9 clearly showed differences in protein expression and function. Additionally, MMP-9 showed high reproducibility in our previous studies[20,47,48]. The present results for MMP-9 suggested that MMP-9 clearly increased even in the early postoperative period after liver surgery and MMP-9 is a major therapeutic target after liver surgery.

TIMPs are also important after liver surgery. Many researchers have focused on TIMP-1 and TIMP-2 during liver regeneration[25-28]. Some researchers have focused on postoperative behavior of TIMP-1[28]. In particular, TIMP-1 has extrahepatic effects during liver failure[23,49-52] and therefore we initially expected that TIMP-1 would show differences in the liver samples. However, zymography for TIMP-1 did not show any differences, although groups with shear stress and portal hypertension (*i.e.*, 60% hepatectomy and 40% SOLT) showed increased protein expression of TIMP-1 in western blotting. TIMP-1 is an endogenous inhibitor of MMP-9 and a balance of MMP-9/TIMP-1 is linked[22,23]. However, the behavior of TIMP-1 in the postoperative liver is still unclear and further studies are required.

Liver damage and apoptotic induction are confirmed even in the early postoperative period after liver surgery but liver injury triggers the liver regeneration cascade after surgery. Once hepatic failure occurs after liver surgery, this damage is usually intractable and fatal. Therefore, the early postoperative period may be a suitable time for treatment to achieve a good postoperative course after liver surgery and our lab focused on OS-mediated damage and the behavior of extracellular matrices after liver surgery[20,48,51,53-56]. The inhibition of apoptotic induction due to OS *via* the ATM/H2AX pathway may be important for a strategy against CIWR injury, even in the condition of sufficient liver volume. Under conditions with insufficient liver remnant, the prevention of apoptotic induction due to OS *via* the Akt/PI3K pathway may be key to improving postoperative course. Also, MMP-9 may be a reliable therapeutic target, especially in the condition of CIWR injury with insufficient liver volume. We hope that our results will be informative for researchers in the hepatology field.

ACKNOWLEDGMENTS

We are grateful to Dennis W Dickson, Monica Castanedes-Casey, Virginia R Phillips, Linda G Rousseau and Melissa E Murray (Department of Neuroscience, Mayo Clinic, Jacksonville, FL, United States) for their technical support with the histopathological evaluation. We are also grateful to Kagemasa Kuribayashi, Takuma Kato, Kanako Saito, Linan Wang, Mie Torii (Department of Cellular and Molecular Immunology, Mie University Graduate School of Medicine, Tsu, Mie, Japan) and Xiangdong Zhao (Innovation Center for Immunoregulation Technologies and Drugs, Transplant Tolerance Unit, Kyoto University Graduate School of Medicine, Kyoto, Japan) for their support with the protein assays and surgical techniques.

COMMENTS

Background

After liver surgery, shear stress with portal hypertension and cold ischemia/warm reperfusion injury trigger the liver regeneration cascade and also cause fatal liver damage.

Research frontiers

Changes and behaviors of oxidative stress and extracellular matrices are still unknown.

Innovations and breakthroughs

Here, the authors investigate the oxidative stress-mediated damage and the behavior of extracellular matrices after liver surgery in various rat models.

Applications

Under conditions with insufficient liver remnant, prevention of oxidative stress-induced damage *via* the Akt/PI3K pathway may be key to improve postoperative course. MMP-9 may be also a therapeutic target after liver surgery.

Terminology

Regulations for oxidative stress and MMP-9 may have a therapeutic potential, in order to resolve the current problems after liver surgery.

Peer review

This is a very interesting paper about the pathophysiology of hepatic failure after hepatectomy and liver transplantation.

REFERENCES

1 **Bachellier P**, Rosso E, Pessaux P, Oussoultzoglou E, Nobili C, Panaro F, Jaeck D. Risk factors for liver failure and mortality after hepatectomy associated with portal vein resection.

Ann Surg 2011; **253**: 173-179 [PMID: 21233614 DOI: 10.1097/SLA.0b013e3181f193ba]
2 **Fan ST**, Mau Lo C, Poon RT, Yeung C, Leung Liu C, Yuen WK, Ming Lam C, Ng KK, Ching Chan S. Continuous improvement of survival outcomes of resection of hepatocellular carcinoma: a 20-year experience. *Ann Surg* 2011; **253**: 745-758 [PMID: 21475015 DOI: 10.1097/SLA.0b013e3182111195]
3 **Lemasters J**, Bunzendahl H, Thurman R. Preservation of the liver. In: Maddrey W, Sorrell M. Transplantation of the liver. 7th ed. East Norwalk: Appleton & Lange, 1995: 297-321
4 **Hori T**, Uemoto S, Gardner LB, Sibulesky L, Ogura Y, Nguyen JH. Left-sided grafts for living-donor liver transplantation and split grafts for deceased-donor liver transplantation: their impact on long-term survival. *Clin Res Hepatol Gastroenterol* 2012; **36**: 47-52 [PMID: 21955515 DOI: 10.1016/j.clinre.2011.08.008]
5 **Busuttil RW**, Goss JA. Split liver transplantation. *Ann Surg* 1999; **229**: 313-321 [PMID: 10077042]
6 **Wang F**, Pan KT, Chu SY, Chan KM, Chou HS, Wu TJ, Lee WC. Preoperative estimation of the liver graft weight in adult right lobe living donor liver transplantation using maximal portal vein diameters. *Liver Transpl* 2011; **17**: 373-380 [PMID: 21445920 DOI: 10.1002/lt.22274]
7 **Ogura Y**, Hori T, El Moghazy WM, Yoshizawa A, Oike F, Mori A, Kaido T, Takada Y, Uemoto S. Portal pressure & lt; 15 mm Hg is a key for successful adult living donor liver transplantation utilizing smaller grafts than before. *Liver Transpl* 2010; **16**: 718-728 [PMID: 20517905 DOI: 10.1002/lt.22059]
8 **Hori T**, Ogura Y, Ogawa K, Kaido T, Segawa H, Okajima H, Kogure T, Uemoto S. How transplant surgeons can overcome the inevitable insufficiency of allograft size during adult living-donor liver transplantation: strategy for donor safety with a smaller-size graft and excellent recipient results. *Clin Transplant* 2012; **26**: E324-E334 [PMID: 22686957 DOI: 10.1111/j.1399-0012.2012.01664.x]
9 **Acuña Castroviejo D**, López LC, Escames G, López A, García JA, Reiter RJ. Melatonin-mitochondria interplay in health and disease. *Curr Top Med Chem* 2011; **11**: 221-240 [PMID: 21244359]
10 **Ghosh N**, Ghosh R, Mandal SC. Antioxidant protection: A promising therapeutic intervention in neurodegenerative disease. *Free Radic Res* 2011; **45**: 888-905 [PMID: 21615270 DOI: 10.3109/10715762.2011.574290]
11 **Turan B**. Role of antioxidants in redox regulation of diabetic cardiovascular complications. *Curr Pharm Biotechnol* 2010; **11**: 819-836 [PMID: 20874678]
12 **Defamie V**, Laurens M, Patrono D, Devel L, Brault A, Saint-Paul MC, Yiotakis A, Barbry P, Gugenheim J, Crenesse D, Dive V, Huet PM, Mari B. Matrix metalloproteinase inhibition protects rat livers from prolonged cold ischemia-warm reperfusion injury. *Hepatology* 2008; **47**: 177-185 [PMID: 18008367]
13 **Ma ZY**, Qian JM, Rui XH, Wang FR, Wang QW, Cui YY, Peng ZH. Inhibition of matrix metalloproteinase-9 attenuates acute small-for-size liver graft injury in rats. *Am J Transplant* 2010; **10**: 784-795 [PMID: 20121733 DOI: 10.1111/j.1600-6143.2009.02993.x]
14 **Hua H**, Li M, Luo T, Yin Y, Jiang Y. Matrix metalloproteinases in tumorigenesis: an evolving paradigm. *Cell Mol Life Sci* 2011; **68**: 3853-3868 [PMID: 21744247 DOI: 10.1007/s00018-011-0763-x]
15 **Overall CM**, López-Otín C. Strategies for MMP inhibition in cancer: innovations for the post-trial era. *Nat Rev Cancer* 2002; **2**: 657-672 [PMID: 12209155]
16 **Alwayn IP**, Verbesey JE, Kim S, Roy R, Arsenault DA, Greene AK, Novak K, Laforme A, Lee S, Moses MA, Puder M. A critical role for matrix metalloproteinases in liver regeneration. *J Surg Res* 2008; **145**: 192-198 [PMID: 18222481 DOI: 10.1016/j.jss.2007.04.002]
17 **Olle EW**, Ren X, McClintock SD, Warner RL, Deogracias MP, Johnson KJ, Colletti LM. Matrix metalloproteinase-9 is an important factor in hepatic regeneration after partial hepatectomy in mice. *Hepatology* 2006; **44**: 540-549 [PMID: 16941692]
18 **Padrissa-Altés S**, Zaouali MA, Franco-Gou R, Bartrons R, Boillot O, Rimola A, Arroyo V, Rodés J, Peralta C, Roselló-Catafau J. Matrix metalloproteinase 2 in reduced-size liver transplantation: beyond the matrix. *Am J Transplant* 2010; **10**: 1167-1177 [PMID: 20353474 DOI: 10.1111/j.1600-6143.2010.03092.x]
19 **Kim TH**, Mars WM, Stolz DB, Michalopoulos GK. Expression and activation of pro-MMP-2 and pro-MMP-9 during rat liver regeneration. *Hepatology* 2000; **31**: 75-82 [PMID: 10613731]
20 **Hori T**, Uemoto S, Hata T, Gardner LB, Chen F, Baine AM, Nguyen JH. Matrix metalloproteinase-9 after the cold ischemia/reperfusion injury and/or shear stress with portal hypertension: an overview. *Surg Today* 2014; **44**: 201-203 [PMID: 23525637]
21 **Ten Hove WR**, Korkmaz KS, op den Dries S, de Rooij BJ, van Hoek B, Porte RJ, van der Reijden JJ, Coenraad MJ, Dubbeld J, Hommes DW, Verspaget HW. Matrix metalloproteinase 2 genotype is associated with nonanastomotic biliary strictures after orthotopic liver transplantation. *Liver Int* 2011; **31**: 1110-1117 [PMID: 21745270 DOI: 10.1111/j.1478-3231.2011.02459.x]
22 **Chirco R**, Liu XW, Jung KK, Kim HR. Novel functions of TIMPs in cell signaling. *Cancer Metastasis Rev* 2006; **25**: 99-113 [PMID: 16680576]
23 **Yamamoto S**, Nguyen JH. TIMP-1/MMP-9 imbalance in brain edema in rats with fulminant hepatic failure. *J Surg Res* 2006; **134**: 307-314 [PMID: 16488444]
24 **Egeblad M**, Werb Z. New functions for the matrix metalloproteinases in cancer progression. *Nat Rev Cancer* 2002; **2**: 161-174 [PMID: 11990853]
25 **Ikebuchi Y**, Ishida C, Okamoto K, Murawaki Y. Association of TIMP-1 and TIMP-2 gene polymorphisms with progression of liver fibrosis in patients with type C chronic liver disease. *Biochem Genet* 2013; **51**: 564-574 [PMID: 23563628 DOI: 10.1007/s10528-013-9587-8]
26 **Rath T**, Menendez KM, Kügler M, Hage L, Wenzel C, Schulz R, Graf J, Nährlich L, Roeb E, Roderfeld M. TIMP-1/-2 and transient elastography allow non invasive diagnosis of cystic fibrosis associated liver disease. *Dig Liver Dis* 2012; **44**: 780-787 [PMID: 22652148 DOI: 10.1016/j.dld.2012.04.008]
27 **Kuyvenhoven JP**, Molenaar IQ, Verspaget HW, Veldman MG, Palareti G, Legnani C, Moolenburgh SE, Terpstra OT, Lamers CB, van Hoek B, Porte RJ. Plasma MMP-2 and MMP-9 and their inhibitors TIMP-1 and TIMP-2 during human orthotopic liver transplantation. The effect of aprotinin and the relation to ischemia/reperfusion injury. *Thromb Haemost* 2004; **91**: 506-513 [PMID: 14983226]
28 **Mohammed FF**, Pennington CJ, Kassiri Z, Rubin JS, Soloway PD, Ruther U, Edwards DR, Khokha R. Metalloproteinase inhibitor TIMP-1 affects hepatocyte cell cycle via HGF activation in murine liver regeneration. *Hepatology* 2005; **41**: 857-867 [PMID: 15726641]
29 **He S**, Atkinson C, Qiao F, Cianflone K, Chen X, Tomlinson S. A complement-dependent balance between hepatic ischemia/reperfusion injury and liver regeneration in mice. *J Clin Invest* 2009; **119**: 2304-2316 [PMID: 19620784 DOI: 10.1172/JCI38289]
30 **Jin X**, Zhang Z, Beer-Stolz D, Zimmers TA, Koniaris LG. Interleukin-6 inhibits oxidative injury and necrosis after extreme liver resection. *Hepatology* 2007; **46**: 802-812 [PMID: 17668886]
31 **Panis Y**, McMullan DM, Emond JC. Progressive necrosis after hepatectomy and the pathophysiology of liver failure after massive resection. *Surgery* 1997; **121**: 142-149 [PMID: 9037225]
32 **Hori T**, Ohashi N, Chen F, Baine AM, Gardner LB, Hata T, Uemoto S, Nguyen JH. Simple and reproducible hepatectomy in the mouse using the clip technique. *World J Gastroenterol* 2012; **18**: 2767-2774 [PMID: 22719184 DOI: 10.3748/wjg.v18.i22.2767]
33 **Hori T**, Nguyen JH, Zhao X, Ogura Y, Hata T, Yagi S, Chen F, Baine AM, Ohashi N, Eckman CB, Herdt AR, Egawa H, Takada Y, Oike F, Sakamoto S, Kasahara M, Ogawa K, Hata

K, Iida T, Yonekawa Y, Sibulesky L, Kuribayashi K, Kato T, Saito K, Wang L, Torii M, Sahara N, Kamo N, Sahara T, Yasutomi M, Uemoto S. Comprehensive and innovative techniques for liver transplantation in rats: a surgical guide. *World J Gastroenterol* 2010; **16**: 3120-3132 [PMID: 20593497]

34 **Hori T**, Uemoto S, Zhao X, Chen F, Baine AMT, Gardner LB, Ohashi N, Conkle F, Castanedes-Casey M, Phillips VR, Rousseau LG, Murray ME, Kamo N, Nguyen JH. Surgical guide including innovative techniques for orthotopic liver transplantation in the rat: Key techniques and pitfalls in whole and split liver grafts. *Ann Gastroentol* 2010; **23**: 270-295

35 **Awasthi YC**, Sharma R, Sharma A, Yadav S, Singhal SS, Chaudhary P, Awasthi S. Self-regulatory role of 4-hydroxynonenal in signaling for stress-induced programmed cell death. *Free Radic Biol Med* 2008; **45**: 111-118 [PMID: 18456001 DOI: 10.1016/j.freeradbiomed.2008.04.007]

36 **Voulgaridou GP**, Anestopoulos I, Franco R, Panayiotidis MI, Pappa A. DNA damage induced by endogenous aldehydes: current state of knowledge. *Mutat Res* 2011; **711**: 13-27 [PMID: 21419140 DOI: 10.1016/j.mrfmmm.2011.03.006]

37 **Irarrazabal CE**, Liu JC, Burg MB, Ferraris JD. ATM, a DNA damage-inducible kinase, contributes to activation by high NaCl of the transcription factor TonEBP/OREBP. *Proc Natl Acad Sci USA* 2004; **101**: 8809-8814 [PMID: 15173573]

38 **Andäng M**, Hjerling-Leffler J, Moliner A, Lundgren TK, Castelo-Branco G, Nanou E, Pozas E, Bryja V, Halliez S, Nishimaru H, Wilbertz J, Arenas E, Koltzenburg M, Charnay P, El Manira A, Ibañez CF, Ernfors P. Histone H2AX-dependent GABA(A) receptor regulation of stem cell proliferation. *Nature* 2008; **451**: 460-464 [PMID: 18185516 DOI: 10.1038/nature06488]

39 **Yuan J**, Adamski R, Chen J. Focus on histone variant H2AX: to be or not to be. *FEBS Lett* 2010; **584**: 3717-3724 [PMID: 20493860 DOI: 10.1016/j.febslet.2010.05.021]

40 **Fernando RN**, Eleuteri B, Abdelhady S, Nussenzweig A, Andäng M, Ernfors P. Cell cycle restriction by histone H2AX limits proliferation of adult neural stem cells. *Proc Natl Acad Sci USA* 2011; **108**: 5837-5842 [PMID: 21436033 DOI: 10.1073/pnas.1014993108]

41 **Fernando RN**, Eleuteri B, Abdelhady S, Nussenzweig A, Andäng M, Ernfors P. Cell cycle restriction by histone H2AX limits proliferation of adult neural stem cells. *Proc Natl Acad Sci USA* 2011; **108**: 5837-5842 [PMID: 21436033 DOI: 10.1073/pnas.1014993108]

42 **Burgering BM**, Coffer PJ. Protein kinase B (c-Akt) in phosphatidylinositol-3-OH kinase signal transduction. *Nature* 1995; **376**: 599-602 [PMID: 7637810]

43 **Franke TF**, Yang SI, Chan TO, Datta K, Kazlauskas A, Morrison DK, Kaplan DR, Tsichlis PN. The protein kinase encoded by the Akt proto-oncogene is a target of the PDGF-activated phosphatidylinositol 3-kinase. *Cell* 1995; **81**: 727-736 [PMID: 7774014]

44 **Haga S**, Ozaki M, Inoue H, Okamoto Y, Ogawa W, Takeda K, Akira S, Todo S. The survival pathways phosphatidylinositol-3 kinase (PI3-K)/phosphoinositide-dependent protein kinase 1 (PDK1)/Akt modulate liver regeneration through hepatocyte size rather than proliferation. *Hepatology* 2009; **49**: 204-214 [PMID: 19065678 DOI: 10.1002/hep.22583]

45 **Khalil A**, Morgan RN, Adams BR, Golding SE, Dever SM, Rosenberg E, Povirk LF, Valerie K. ATM-dependent ERK signaling via AKT in response to DNA double-strand breaks. *Cell Cycle* 2011; **10**: 481-491 [PMID: 21263216]

46 **Maulik N**, Das DK. Emerging potential of thioredoxin and thioredoxin interacting proteins in various disease conditions. *Biochim Biophys Acta* 2008; **1780**: 1368-1382 [PMID: 18206121 DOI: 10.1016/j.bbagen.2007.12.008]

47 **Nguyen JH**, Yamamoto S, Steers J, Sevlever D, Lin W, Shimojima N, Castanedes-Casey M, Genco P, Golde T, Richelson E, Dickson D, McKinney M, Eckman CB. Matrix metalloproteinase-9 contributes to brain extravasation and edema in fulminant hepatic failure mice. *J Hepatol* 2006; **44**: 1105-1114 [PMID: 16458990]

48 **Ohashi N**, Hori T, Chen F, Jermanus S, Eckman CB, Nakao A, Uemoto S, Nguyen JH. Matrix metalloproteinase-9 contributes to parenchymal hemorrhage and necrosis in the remnant liver after extended hepatectomy in mice. *World J Gastroenterol* 2012; **18**: 2320-2333 [PMID: 22654423 DOI: 10.3748/wjg.v18.i19.2320]

49 **Chen F**, Radisky ES, Das P, Batra J, Hata T, Hori T, Baine AM, Gardner L, Yue MY, Bu G, del Zoppo G, Patel TC, Nguyen JH. TIMP-1 attenuates blood-brain barrier permeability in mice with acute liver failure. *J Cereb Blood Flow Metab* 2013; **33**: 1041-1049 [PMID: 23532086 DOI: 10.1038/jcbfm.2013.45]

50 **Nguyen JH**. Blood-brain barrier in acute liver failure. *Neurochem Int* 2012; **60**: 676-683 [PMID: 22100566 DOI: 10.1016/j.neuint.2011.10.012]

51 **Chen F**, Hori T, Ohashi N, Baine AM, Eckman CB, Nguyen JH. Occludin is regulated by epidermal growth factor receptor activation in brain endothelial cells and brains of mice with acute liver failure. *Hepatology* 2011; **53**: 1294-1305 [PMID: 21480332 DOI: 10.1002/hep.24161]

52 **Nguyen JH**. Subtle BBB alterations in brain edema associated with acute liver failure. *Neurochem Int* 2010; **56**: 203-204; author reply 205-207 [PMID: 20201130]

53 **Hori T**, Gardner LB, Chen F, Baine AM, Hata T, Uemoto S, Nguyen JH. Liver graft pretreated in vivo or ex vivo by γ-aminobutyric acid receptor regulation. *J Surg Res* 2013; **182**: 166-175 [PMID: 23010512 DOI: 10.1016/j.jss.2012.08.055]

54 **Hori T**, Gardner LB, Hata T, Chen F, Baine AM, Uemoto S, Nguyen JH. Pretreatment of liver grafts in vivo by γ-aminobutyric acid receptor regulation reduces cold ischemia/warm reperfusion injury in rat. *Ann Transplant* 2013; **18**: 299-313 [PMID: 23792534 DOI: 10.12659/AOT.883955]

55 **Ohashi N**, Hori T, Chen F, Jermanus S, Nakao A, Uemoto S, Nguyen JH. Matrix metalloproteinase-9 in the initial injury after hepatectomy in mice. *World J Gastroenterol* 2013; **19**: 3027-3042 [PMID: 23716982 DOI: 10.3748/wjg.v19.i20.3027]

56 **Gardner LB**, Hori T, Chen F, Baine AM, Hata T, Uemoto S, Nguyen JH. Effect of specific activation of γ-aminobutyric acid receptor in vivo on oxidative stress-induced damage after extended hepatectomy. *Hepatol Res* 2012; **42**: 1131-1140 [PMID: 22583816 DOI: 10.1111/j.1872-034X.2012.01030.x]

P- Reviewer: Hashimoto N **S- Editor**: Zhai HH
L- Editor: Roemmele A **E- Editor**: Liu XM

百世登

Baishideng®

Published by **Baishideng Publishing Group Co., Limited**
Flat C, 23/F., Lucky Plaza,
315-321 Lockhart Road, Wan Chai, Hong Kong, China
Fax: +852-65557188
Telephone: +852-31779906
E-mail: bpgoffice@wjgnet.com
http://www.wjgnet.com

ANNALS OF TRANSPLANTATION

ORIGINAL PAPER

ISSN 1425-9524
© Ann Transplant, 2014; 19:519-536
DOI: 10.12659/AOT.890890

Received: 2014.04.19
Accepted: 2014.07.08
Published: 2014.10.17

Induction of Alloantigen-specific CD4+ T Regulatory Type 1 Cells by Alloantigen Immunization and Ultraviolet-B Irradiation: A Pilot Study in Murine Transplantation Models With Skin and Cardiac Allografts

Authors' Contribution:
Study Design A
Data Collection B
Statistical Analysis C
Data Interpretation D
Manuscript Preparation E
Literature Search F
Funds Collection G

BCD 1,2 Tomohide Hori
A 2 Kagemasa Kuribayashi
B 2,3 Kanako Saito
B 2 Linan Wang
B 2 Mie Torii
A 1 Shinji Uemoto
A 2 Takuma Kato

1 Department of Transplant Surgery, Kyoto University Hospital, Kyoto, Japan
2 Department of Cellular and Molecular Immunology, Mie University Graduate School of Medicine, Tsu, Japan
3 Department of Hematology and Oncology, Mie University Hospital, Tsu, Japan

Corresponding Author: Tomohide Hori, e-mail: horit@kuhp.kyoto-u.ac.jp
Source of support: This study was supported by a Grant-in-Aid for Scientific Research (C, No. 20591523) from the Japanese Ministry of Education, Culture, Sports, Science and Technology, and the Japanese Society for the Promotion of Science

Background: The use of ultraviolet (UV)-B irradiation after alloantigen immunization is unknown because previous studies focused on UV-B irradiation before immunization. Here, we investigated immunosuppressive effects induced by UV-B irradiation after immunization, and examined the phenotype of induced regulatory T cells and the possible mechanism of induction.

Material/Methods: B6 mice (H-2^b) were intravenously immunized by splenocytes from CBF1 mice (H-$2^{b/d}$). One week after alloantigen immunization, B6 mice received high-dose UV-B irradiation (40 kJ/m^2). Four weeks after UV-B irradiation, proliferation assays (n=4, in each), transplantations with skin or cardiac allografts (n=5, in each), cytokines in mixed lymphocyte culture (n=6, in each), and adoptive transfer of CD4+ T cells to naïve B6 mice (n=5, in each) were performed. Mice were divided into 4 groups: untreated control, immunized control, UV-irradiated control, and an immunized and UV-irradiated group. B6C3F1 mice (H-$2^{b/k}$) were used as irrelevant alloantigen with immunization controls. Anti-IL-10 monoclonal antibody was used to block IL-10 before and after UV-B irradiation.

Results: Immune responses against the immunizing antigen were markedly suppressed in immunized and UV-irradiated mice in an alloantigen-specific manner. Surprisingly, CD4+ T cells from immunized and UV-irradiated mice produced significantly larger amounts of IL-10, in an alloantigen-specific manner. Moreover, alloantigen-specific immunosuppression via CD4+ regulatory T cells was transferable to naïve B6 mice. IL-10 blocking clearly abrogated alloantigen-specific immunosuppression, indicating that UV-B irradiation evoked T regulatory type 1 cells.

Conclusions: This study demonstrates for the first time that immunization and UV irradiation induces alloantigen-specific CD4+ T regulatory type 1 cells, and that IL-10 plays an important role for this induction.

MeSH Keywords: **Allografts • Liver Transplantation • T-Lymphocytes, Regulatory • Transplantation Immunology • Ultraviolet Rays**

Full-text PDF: http://www.annalsoftransplantation.com/abstract/index/idArt/890890

6534 — 10 89

Background

Ultraviolet (UV) light, especially the mid-wave range (UV-B, 280–320 nm), is an important environmental factor that affects human health [1–5]. Although primary carcinogenesis is the most common problem, UV irradiation impairs immune responses to oncologic and infectious antigens [1,4,6]. Paradoxically, immunosuppressive effects induced by UV irradiation may have therapeutic potential for autoimmune diseases or host-versus-graft rejection [1,3,4,7–12]. Thus, UV-B irradiation is associated with clinical benefits.

Immunosuppressants have revolutionized clinical transplantation, but also cause pan-immunosuppressive effects [13]. Regulatory T cells (Tregs) are important in immunity [14–17], and alloantigen-specific immunosuppression is critical for organ transplantation [7,10,16,18–20]. To date, our group has focused on applications of UV irradiation [21–25]. To induce alloantigen-specific Tregs, high-dose UV-B irradiation accompanied by alloantigen immunization is required [5,7,10,11,26–29]. In the late 1980s, many studies reported that antigen-specific Tregs were induced by high-dose UV-B irradiation before antigen immunization [7,10,11,26], because it was thought that UV irradiation-induced alternation/modulation of antigen-presenting cell (APC) functions were required for antigen-specific Treg induction [1,7,10,26,29–32].

The focus of our research group is to assess the application of alloantigen-specific immunosuppression in murine transplantation models. The immune effect of UV-B irradiation after alloantigen immunization has not been established. Here, we investigated the use of UV-B irradiation after alloantigen immunization to induce alloantigen-specific immunosuppression, and investigated the mechanism and phenotype of induced Tregs.

Material and Methods

Animals

UV-irradiated mice are a useful model to investigate antigen-specific immunosuppression [7,10]. C57BL/6 (B6, H-2^b), (BALB/c×C57BL/6)F_1 (CBF1, H-$2^{b/d}$), and (C57BL/6×C3H/HeN)F_1 (B6C3F1, H-$2^{b/k}$) mice were obtained from Japan SLC (Hamamatsu, Japan). These mice were maintained in a specific pathogen-free facility for laboratory animals at Mie University Graduate School of Medicine in accordance with institutional guidelines for animal welfare. To unify age and sex, 6-week-old female mice were used at the time of the first experimental procedure.

Study design and ethical approval

Study design is summarized in Figure 1. Although graft-versus-host disease is intractable in the field of bone marrow transplantation, host-versus-graft reaction and systemic immunoresponse are important for organ transplantation. Here, we mainly focused on organ transplantation to reduce post-transplant rejection. Therefore, we set a semi-allogeneic combination (not a full-allogeneic combination) in the model with delayed-type hypersensitivity (DTH). All experimental procedures, including animal care, were approved by the Ethics Review Committee for Animal Experimentation of Mie University Graduate School of Medicine (No. 3106), based on the Ethics Guidelines of the Declaration of Helsinki.

Immunization with alloantigen

Spleens were removed from naïve CBF1 mice (H-$2^{b/d}$). Splenocytes were freshly isolated, and resuspended in phosphate-buffered saline (PBS). A total of 2×10^7 cells/0.5 ml of single-cell splenocytes were intravenously injected into individual age- and sex-matched naïve B6 mice (H-2^b) via the lateral tail vein.

Immunization with dendritic cells

Bone marrow-derived mature dendritic cells (DC) were obtained from naïve CBF1 mice (H-$2^{b/d}$). Both thighbones were flushed with Hanks' solution to obtain bone marrow cells. Red blood cells and T cells were depleted by sorting system (Dynal magnetic beads, Invitrogen, Life Technologies, Carlsbad, CA, USA). Culture medium comprised complete Roswell Park Memorial Institute (RPMI) medium (RPMI 1640, Nissui Pharmaceutical Co., Taito, Tokyo, Japan) supplemented with 10% fetal calf serum (FCS) (JRH Biosciences, Lenexa, KS, USA) and 0.5 mM 2-mercaptoethanol (2-ME). Sterile flat-bottomed 6-well plates (Nunclon™ ΔSurface, Sigma-Aldrich, St. Louis, MO, USA) were used for cell culture. A total of 6×10^6 cells/3 ml/well were cultured at 37°C. Granulocyte-macrophage colony-stimulating factor (GM-CSF) (500 U/0.5 ml) was added. Medium change and GM-CSF addition were performed on days 1-3, 5, and 7. Mature DC were obtained at day 8 by cell sorting (AutoMACS program; Miltenyi Biotec Inc., Auburn, CA, USA). Expression of MHC class II and CD11c were analyzed by flow cytometry, and the purity of DC was maintained at >90%. Age- and sex-matched naïve B6 mice (H-2^b) were immunized by intravenous injection of mature DC (2×10^6 cells/0.5 ml/mouse).

UV-B irradiation after alloantigen immunization

One week after alloantigen immunization, immunized B6 mice received UV-B irradiation. The UV source was a bank of 3 unfiltered UV lamps (UVP Inc., Upland, CA, USA) with an emission spectrum in the UV-B range (280–320 nm). The mean UV-B irradiation was 2372 mJ/cm²/h. A 10-cm² area of the ventral skin was carefully shaved without injury to the abdominal wall. To prevent unevenness of UV-B irradiation, the feet of

Indexed in: [Science Citation Index Expanded] [Index Medicus/MEDLINE] [Chemical Abstracts] [Scopus]

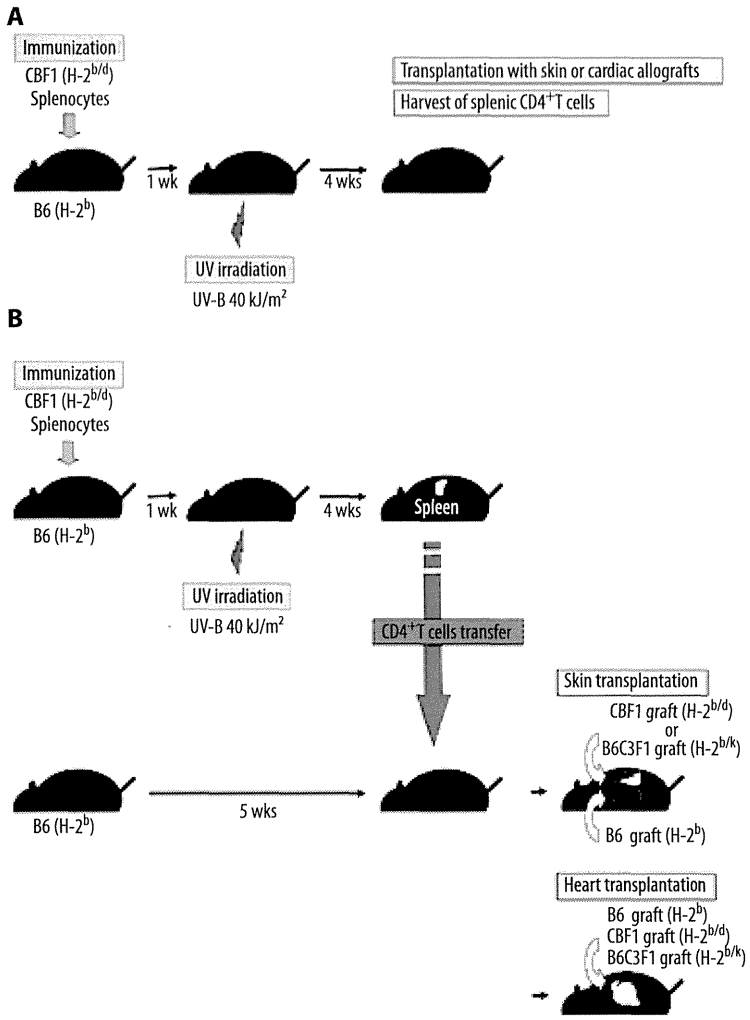

Figure 1. Study design. (**A**) Naïve B6 mice (H-2^b) were intravenously immunized with splenocytes from naïve CBF1 mice (H-$2^{b/d}$) (2×10^7 cells/0.5 ml/mouse). Immunized B6 mice received UV-B irradiation at a dose of 40 kJ/m^2. At 4 weeks after UV irradiation, harvest of splenic CD4$^+$T cells and allograft transplantations were performed. (**B**) Splenic CD4$^+$T cells were purified from immunized and UV-irradiated mice at 4 weeks after UV irradiation. These CD4$^+$T cells were transferred into age- and sex-matched naïve B6 mice. Transferred mice received allografts immediately.

anesthetized mice were fixed to a metallic halftone plate by silk threads. Thus, the shaved abdominal wall was sufficiently extended and exposed equally to the UV lamps. The backs of mice, which were required for graft beds, were protected from UV irradiation.

Cell preparation of stimulator cells

To prevent cytokine release from stimulator T cells and proliferation of the stimulator T cells themselves, X-irradiated and T cell-depleted single splenocytes from naïve CBF1 (H-$2^{b/d}$) and B6C3F1 (H-$2^{b/k}$) mice were prepared. To deplete T cells, single splenocytes were incubated with anti-Thy1.2 magnetic beads (Anti-Mouse CD90.2 [Thy-1.2] Particles-DM; BD Biosciences, Franklin Lakes, NJ, USA), and the procedures for T cell depletion were performed using a sorting system (BD IMag system; BD Biosciences). T cell-depleted single splenocyte suspensions were X-irradiated at a dose of 28 Gy.

Mixed lymphocyte reactions

One-way allogeneic mixed lymphocyte reactions (MLR) were performed as proliferation assays in sterile flat-bottomed 96-well plates for 96 h at 37°C. All cultures were set up in triplicate. Culture medium comprised complete RPMI medium supplemented with 10% FCS, 0.5 mM 2-ME, and streptomycin. Unfractionated single splenocytes from B6 mice (5×10^5 cells) were cultured with either CBF1 or B6C3F1 stimulator cells (5×10^5 cells) in a total volume of 250 µl of culture medium in 96-well plates for 96 h at 37°C. The cultures were pulsed with 1 µCi/well of [^{3}H]-thymidine for the last 12 h of a 96-h culture and harvested onto glass fiber filters. Proliferation was measured by [^{3}H]-thymidine incorporation using liquid scintillation counting (counts per minute).

Skin transplantation

A whole-layer graft of tail skin was transplanted onto graft beds on the backs of recipient mice by microsurgery (×16

Indexed in: [Science Citation Index Expanded] [Index Medicus/MEDLINE] [Chemical Abstracts] [Scopus]

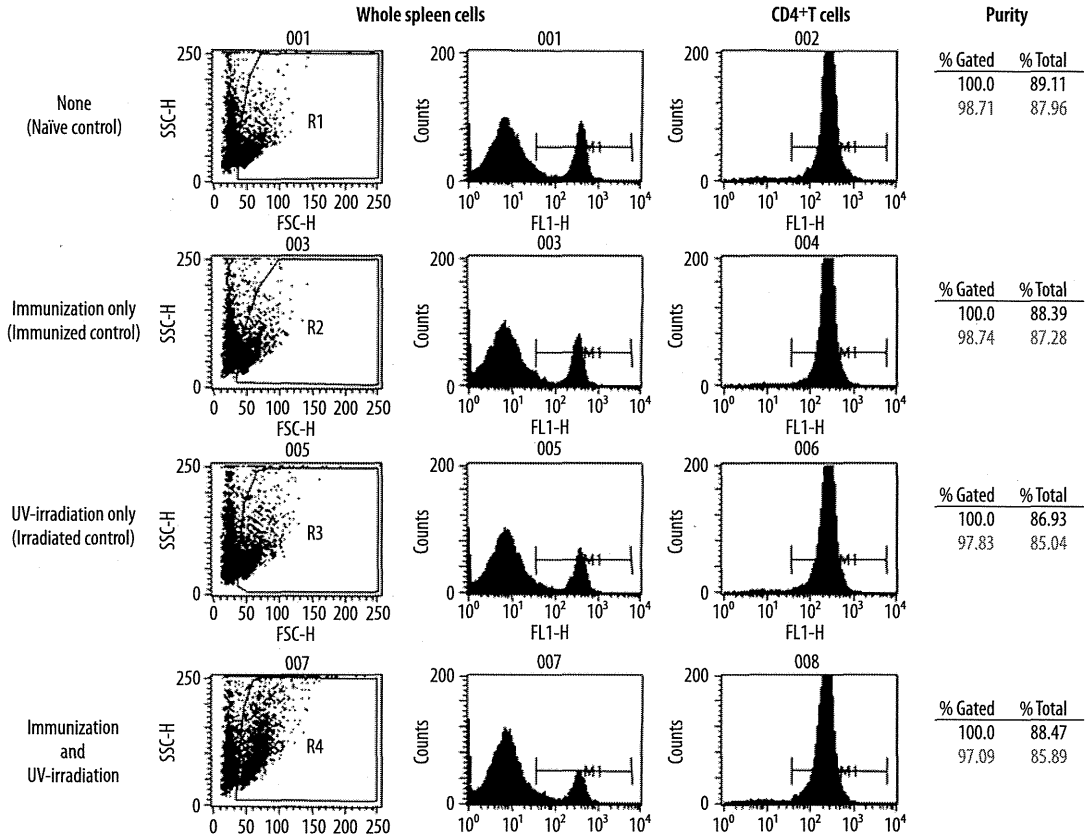

Figure 2. Purities of sorted CD4+T cells. Sorted splenic CD4+T cells routinely contained >95% of CD4+T cells (red).

magnification). Skin grafts were harvested from age- and sex-matched donor mice. All grafts were unified to an area of 10×5 mm to allow the quantitative uniformity of alloantigens. Under anesthesia, a syngeneic graft was transplanted onto the left- side back, while an allogeneic graft was grafted onto the right-side back. Transplanted grafts were wrapped in a sterile bandage with an antibiotic ointment. Transplanted recipient mice were placed in separate cages to avoid scratching of transplanted grafts by cage mates. They were fed with a supply of Ringer's lactate solution. Transplanted grafts were monitored every day after bandage removal at day 7. Graft rejection was defined as >90% necrosis of graft epithelium [25,33].

Heart transplantation

As the second model, to confirm immunosuppressive effects *in vivo*, heterotopic heart transplantation was employed. Cardiac grafts were harvested from age- and sex-matched donor mice. Cardiac grafts were ectopically transplanted to recipient mice. Surgical procedures, including ultra-microsurgery, were described previously [34]. Ultra-microsurgical procedures were performed under ×20 magnification (Surgical Scope M680, Type 10445496; Leica Microsystems Inc., Bannockburn, IL, USA). Transplanted mice were placed in separate cages, and fed with a supply of Ringer's lactate solution. Graft rejection was defined as no palpable pulsation of heterotopic graft [28,35].

Cell preparation of splenic CD4+T cells

To prepare CD4+T cells, spleens were harvested from B6 mice. Single-cell suspensions of whole splenocytes (1×10^7 cells) were incubated with CD4 microbeads (CD4 [L3T4] MicroBeads; Miltenyi Biotec, Inc.) and positively selected over separation columns (AutoMACS program; Miltenyi Biotec, Inc.). To achieve a high purity of CD4+T cells, splenocytes were filtrated through the separation columns twice, although the total amount of sorted CD4+T cells was decreased. Purities of sorted CD4+T cells routinely contained >95% CD4+T cells (Figure 2).

Mixed lymphocyte cultures (MLC)

Culture medium comprised complete RPMI medium supplemented with 10% FCS and 0.5 mM 2ME. Stimulator cells from naïve CBF1 and B6C3F1 mice were suspended in culture

Indexed in: [Science Citation Index Expanded] [Index Medicus/MEDLINE] [Chemical Abstracts] [Scopus]